Article:

Voutsa, V., Turnbull, L., Parsons, A. et al. (2026) Large scale connectivity of river networks during rainfall events. Water Resources Research, 62 (7). e2025WR041408. ISSN: 0043-1397

https://doi.org/10.1029/2025wr041408

AGU ADVANCING EARTH AND SPACE SCIENCES

Water Resources Research

RESEARCH ARTICLE
10.1029/2025WR041408

Large Scale Connectivity of River Networks During Rainfall Events

Venetia Voutsa[1], Laura Turnbull[2], Antony Parsons[3], John Wainwright[2], and Marc-Thorsten Hütt[1]

[1]School of Science, Constructor University Bremen, Bremen, Germany, [2]Department of Geography, Durham University, Durham, UK, [3]Department of Geography, University of Sheffield, Sheffield, UK

Key Points:

- We introduce an event-scale network framework to quantify river connectivity by integrating structural (SC) and functional (FC) analyses
- We apply Generalized Additive Model modeling and hierarchical clustering to link SC-FC patterns with rainfall characteristics and discharge
- Large events show high sequential SC-FC correlations, indicating system-wide flow, while small intense storms yield localized connectivity

Supporting Information:

Supporting Information may be found in the online version of this article.

Correspondence to:

V. Voutsa,
vvoutsa@constructor.university

Citation:

Voutsa, V., Turnbull, L., Parsons, A., Wainwright, J., & Hütt, M.-T. (2026). Large scale connectivity of river networks during rainfall events. *Water Resources Research*, *62*, e2025WR041408. https://doi.org/10.1029/2025WR041408

Received 20 JUN 2025
Accepted 16 JUN 2026

Author Contributions:

Conceptualization: Venetia Voutsa, Laura Turnbull, Antony Parsons, John Wainwright, Marc-Thorsten Hütt
Data curation: Venetia Voutsa, Laura Turnbull
Formal analysis: Venetia Voutsa, Laura Turnbull
Funding acquisition: Antony Parsons
Investigation: Venetia Voutsa, Laura Turnbull
Methodology: Laura Turnbull
Software: Laura Turnbull
Supervision: Laura Turnbull, Antony Parsons, John Wainwright, Marc-Thorsten Hütt

Abstract River connectivity is essential for maintaining fertile floodplains, healthy ecosystems, and human activities, particularly in semi-arid regions, where water flow is often intermittent. Despite its importance, very few studies have attempted to quantify connectivity at the scale of individual rainfall-runoff events. In this study, we present a novel framework for exploring synchronous and sequential connectivity to capture the hydrological response of a system. We distinguish between structural (SC) and functional (FC) connectivity by constructing structural networks utilizing topographic data from the Walnut Gulch Experimental Watershed in Arizona, USA, and correlation-based functional networks using high-resolution runoff data. We examine how SC-FC relations vary across events and how they relate to the hydrological responses of the system. We classify rainfall events via unsupervised clustering and identify the corresponding dominant runoff connectivity patterns within each cluster. The results of our analysis showed that short, intense storms tend to produce localized runoff connectivity, characterized by dominant synchronous SC-FC relations, whereas larger rainfall events tend to exhibit higher sequential SC-FC correlation values, indicating widespread system connectivity. Furthermore, our analysis revealed that there is a minimum threshold in the synchronous connectivity value (0.13), before positive sequential activity appears in the system. Comparable synchronous and sequential connectivity values typically indicate that water flow reached the watershed outlet; however, maximum SC-FC value is not necessarily associated with peak discharge at the watershed outlet. Due to its flexibility, our approach suggests a general framework for analyzing connectivity in any river network with an ephemeral flow regime.

1. Introduction

Watersheds are an example of a complex system, where the hydrological response to a rainfall input can be non-linear and non-stationary. A given response at the watershed outlet may arise through different spatial and temporal patterns of flow within the watershed; hence the hydrological response at a watershed outlet might be achieved through different processes and pathways (Khatami et al., 2019). Conversely, similar rainfall amounts may give rise to different patterns and amounts of flow, depending on the location and timing of the rainfall and antecedent conditions. As a result, there may not be a one-to-one link between hydrological response at a watershed outlet and a set of functional relations between elements of the watershed leading to that response (Parsons et al., 2025). Local factors controlling the hillslope-scale runoff response (e.g., soil, vegetation, slope), in combination with river network topology, play a central role in structuring the hydrological behavior that emerges at larger spatial scales (Benda & Bigelow, 2014; Benda et al., 2004; Czuba & Foufoula-Georgiou, 2015). As such, watersheds are a classic example of a complex system, where the collective system behavior arises through dynamical and often non-linear relations across multiple spatial and temporal scales (Sivakumar & Singh, 2012; Xu et al., 2010). These characteristics make understanding the behavior of these systems particularly challenging in the absence of approaches that allow us to explore these dynamical relations (Turnbull et al., 2018).

The functional relations between elements of a watershed can be described by their connectivity, which is an important emergent property of hydrological systems that influences (and is influenced by) the translation of the small-scale hydrological response to larger spatial scales, impacting the magnitude of sediment, nutrient and pollutant transport (Brinkerhoff, 2024), groundwater recharge and flooding (Baillie et al., 2007; Goodrich et al., 2004, 2018), as well as geomorphological (Bull, 1997; Hooke, 2022), ecological and riparian processes (Snyder & Williams, 2000; Tiwari et al., 2024).

Connectivity is especially important in drylands, where river flow tends to be ephemeral or intermittent, as a result of infrequent rainfall. Short-timescale fluctuations in river connectivity play an important role because they create

Validation: Laura Turnbull, Antony Parsons
Visualization: Venetia Voutsa, Laura Turnbull
Writing – original draft: Venetia Voutsa, Laura Turnbull
Writing – review & editing: Venetia Voutsa, Laura Turnbull, Antony Parsons, John Wainwright, Marc-Thorsten Hütt

brief but critical windows that control movement, survival, and local persistence of organisms: temporal links allow dispersal, recolonization, and population mixing, so biodiversity patterns and metacommunity dynamics depend on these pulsed connections (Datry et al., 2023). These brief connectivity pulses also drive pulses of water, sediment and nutrients downstream, so short-term connectivity governs the timing and magnitude of biogeochemical fluxes and water-quality responses that affect the existence and the function of the ecosystems (Harvey et al., 2019). Process-based hydrological modeling shows that these brief connectivity pulses are shaped by rainfall, groundwater dynamics, and catchment morphology (Zanetti et al., 2024). Active stream networks expand and contract over hours to days, creating dynamic pathways that control both organism movement and the transport of water, sediments, and nutrients. Capturing these rapid fluctuations is therefore key to understanding ecosystem structure, function, and responses to hydrological variability. Furthermore, because management actions (e.g., flow regulation, habitat restoration, pollution mitigation) and monitoring programs are implemented on specific temporal cycles, neglecting the rapid dynamics of short-timescale hydrological connectivity can lead to mistimed actions and misinterpretation of ecological indicators. These considerations underscore the necessity of integrating short-term connectivity metrics into both ecological assessments and operational planning to support more effective river management (Garbin et al., 2019).

Previous research has highlighted the sensitivity of the runoff response to rainfall characteristics in drylands. The location, magnitude, and spatial extent of rainfall events are important controls on runoff generation on hillslopes and small-scale headwater catchments (Chouksey et al., 2017; Freeze, 1980; Goodrich et al., 1995). At larger spatial scales, the size of the storm core (locations with particularly high rainfall amounts over a sustained period) is a more important predictor of the runoff response (Goodrich et al., 1997). Whilst the effect of rainfall variability in time and space on the translation of the small-scale runoff response to larger spatial scales is recognized as being important (Zhao et al., 2022), it nevertheless remains less understood than small-scale processes (Meles et al., 2024). The functional relations between different elements of a watershed depend on a multitude of factors; spatial variations in rainfall across a watershed, local conditions such as soil, vegetation and slope, the contributing area to different locations, the location within the larger network, the timing and magnitude of flow from tributaries into the main channel network, the influence of transmission losses–which are known to increase with an increase in contributing area (Goodrich et al., 1997)-all contribute into how functional connectivity is shaped. Hence, in drylands, connectivity is event-driven rather than continuous meaning that quantifying and understanding the hydrological connectivity of flow within these systems requires an approach that can deal with their unique characteristics. However, existing quantitative approaches are only few and not well suited to ephemeral systems with short-duration flow. In particular, traditional approaches are largely developed for perennial rivers, where flow is continuous (Boulton et al., 2017), in contrast to ephemeral and intermittent systems characterized by frequent transitions between flowing and non-flowing phases, episodic runoff generation, and strong variability in flow discharge. Many of the existing methodologies assume continuous water flow and combined with the scarcity of measured data in ephemeral catchments have contributed to limited development of quantitative frameworks to assess hydrological connectivity in such systems.

It has become conventional to distinguish between structural and functional connectivity (see extensive reviews in Dwivedi et al., 2025; Crompton et al., 2023; Wainwright et al., 2011). Structural connectivity describes the topology upon which hydrological processes occur, and functional connectivity quantifies flow connectivity between different parts of hillslopes or river systems (Deng et al., 2018; Tiwari et al., 2025). Conceptualization of connectivity has also developed to explore the couplings between different drivers, known as process connectivity (Deng et al., 2018; Passalaqua, 2016) and it has been explored within a range of different environmental contexts, including deltas (Passalaqua, 2016; Sendrowski & Passalacqua, 2017) and rivers (Lu, 2024).

A range of approaches has been used to characterize and quantify structural and functional connectivity. Wohl (2017) and Deng et al. (2018) evaluated functional connectivity in a downstream direction by calculating differences in fluctuations of water level between adjacent stations, using daily hydrological data with a specified time lag. Their approach enabled analysis of continuous changes over time and the detection of abrupt changes in functional connectivity. The work of Lu (2024) used an information-theory approach to measure the connections in water levels over time. The study found that structural connectivity plays a crucial role in enhancing process connectivity. Additionally, it highlighted the importance of highly synchronized flow dynamics in upstream areas for increasing flow connectivity downstream. Although these recent developments have contributed to the advancement of quantifying and exploring functional connectivity in river networks, tools for systematically investigating functional connectivity at relevant timescales for short-duration flow events in ephemeral systems are still lacking.

Given the inherent structure of river networks and the available tools for analyzing complex systems, networks-the representation of a system as a graph consisting of nodes, that is, the elements of the system and edges, that is, a set of connecting links—provide a natural framework for studying connectivity in river systems (Tejedor et al., 2015). A range of studies have used networks to investigate the topological properties of river. For example, networks have been widely used to analyze connectivity in braided rivers (Howard et al., 1970), to explore ecological dynamics (Recinos et al., 2024) and optimal channel networks (Briggs & Krishnamoorthy, 2013; Rigon et al., 1993). The wide-ranging use of networks to study various aspects of hydrological systems stems from their flexibility. Networks enable an effective representation of connectivity of complex systems and a detailed analysis of interactions between system components at the scale of individual nodes and across the entire network (Tejedor et al., 2015; Tiwari et al., 2025).

Analysis of complex systems using networks extends far beyond the reach of hydrology, and indeed, novel developments have been made in hydrology by capitalizing on developments made in other disciplines. From a theoretical perspective, Voutsa et al. (2021) explored how dynamics on graphs shape functional connectivity under various conditions and identified two classes of connectivity: simultaneous functional connectivity FC_{sim} or equivalently synchronous functional connectivity, FC_{sync}, which assesses the extent to which nodes within a network are co-activated (i.e., display same or similar dynamical behavior), and sequential functional connectivity (FC_{seq}) (sometimes referred in hydrology as longitudinal functional connectivity (Deng et al., 2018)), which assesses the time-delayed activity of nodes within a network (e.g., the propagation of flow in a downstream direction) (Voutsa et al., 2021).

In this study, we characterize event-scale connectivity in Walnut Gulch Experimental Watershed (WGEW), based on the approach outlined in Voutsa et al. (2021), where they compared the degree of similarity between structural and functional connectivity matrices, that is, the SC - FC correlation. We show how the two types of SC - FC relations vary across individual events and we examine whether there are unique signatures of SC - FC correlations for different types of rainfall events. This novel approach allows us to quantify the relative roles of rainfall characteristics in driving synchronous and sequential connectivity, and to identify the conditions under which amplified hydrological responses and large spatial scales of connection occur. In a highly episodic, semi-arid system such as the WGEW, these insights are crucial for understanding how runoff generation and sediment transport propagate through the drainage network. Under projected changes in the spatial and temporal distribution of rainfall, an improved understanding of connectivity will be particularly important for anticipating how such systems may respond in the future.

2. Materials and Methods

2.1. Study Area

The WGEW, located in southeast Arizona, USA, is a 148 km^2 ephemeral watershed located in the transition zone between the Sonoran and Chihuahuan deserts that drains into the San Pedro river (Figure 1). The WGEW is extensively instrumented with 88 rain gauges to monitor rainfall, and 22 flumes to measure runoff and erosion at high temporal resolutions and across a range of spatial scales (Meles et al., 2022; Nichols, 2019). Detailed measurements of rainfall and runoff, as well as extensive spatial data sets (Heilman et al., 2008) and high-resolution topographic data allow for a detailed quantification of structural and functional connectivity. In our analysis we considered the data from 81 raingauges and 19 flumes. The selection was made based on the consistency of their operation during the years 2000–2024 and the correspondence between them, in terms of recorded rainfall (by raingauges) contributing into the runoff measurements of specific flumes (Tables 1 and 2 give summaries).

The main channel through the watershed is incised into alluvial fill, which facilitates transmission loss into the channel bed. Transmission loss is a key process influencing the connectivity of flow downstream and the magnitude of the flood peak, and becomes increasingly important with an increase in drainage area (Goodrich et al., 1997). In the WGEW there are stock ponds that may intercept runoff during small or moderate rainfall events, restricting the connectivity and potentially preventing the water flow from reaching flume 1. During larger

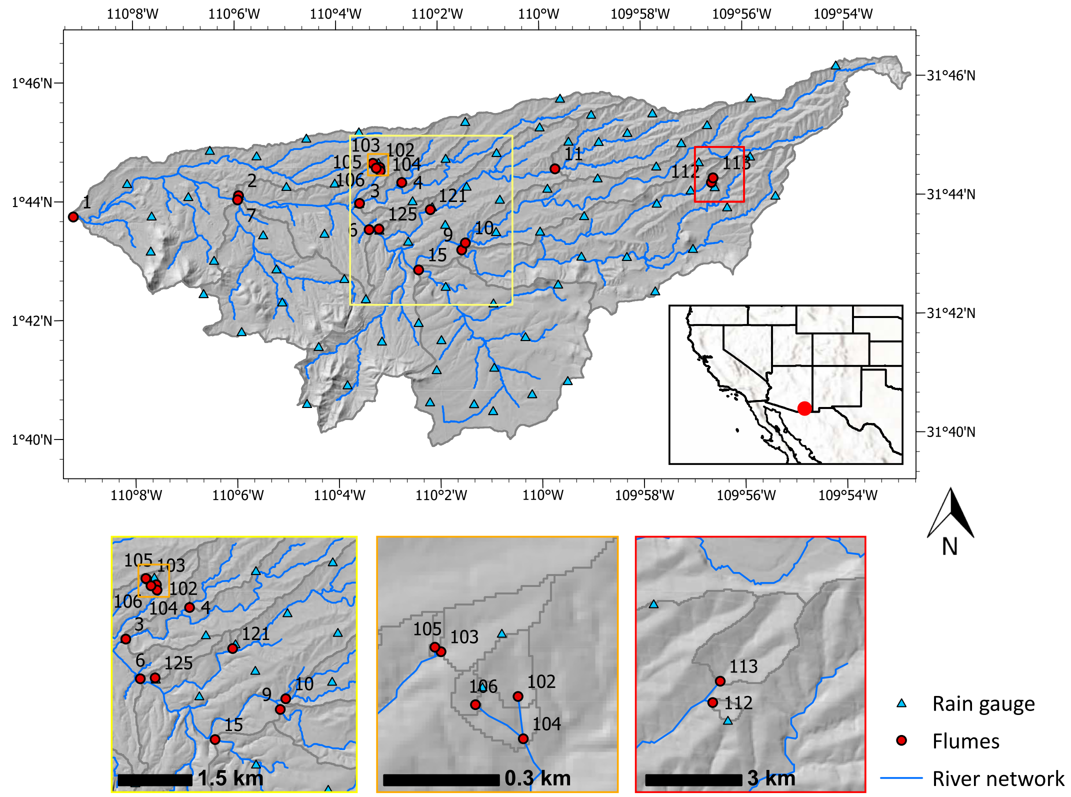

Figure 1. Map of the Walnut Gulch Experimental Watershed, showing its location in the southwestern USA, the distribution of rain gauges, location of flumes (and their corresponding ID) along the river network, and the contributing area to each flume.

events, however, the stock ponds may overflow, allowing water to reach the watershed outlet (see detailed description and their impact on connectivity in Supporting Information S1).

The annual average rainfall across WGEW is roughly 312 mm, with approximately 60% falling during the summer monsoon (Goodrich et al., 2008). This distinct seasonality is driven by convective rainfall events, associated with an inflow of atmospheric moisture associated with the North American monsoon. Winter rainfall is characterized by low-intensity rainfall associated with Pacific Ocean moisture and the southerly displacement of the jet stream (Sheppard et al., 2002).

2.2. Data and Data Preprocessing

For this study, we downloaded, preprocessed, used and analyzed the open access precipitation and runoff event data from the year 2000 onwards, when the measurements are digital (Nichols & Anson, 2008). The raw data were downloaded from the website USDA Agricultural Research Service, Southwest Watershed Research Center (2025).

To implement an event-scale connectivity analysis, the runoff data were grouped into distinct, temporally defined events, as follows: we grouped sequential runoff measurements of the activated flumes into an event until there was a time gap of 2 hr in the recorded measurements. In intermittent systems, events are typically inherently independent, as water flow within the channels occurs only after rainfall and when other conditions are conducive for runoff generation. Therefore, there are discrete temporal intervals during which there is runoff generation. The threshold for the minimum inter-event time should be defined in a system-oriented manner, during the data preprocessing stage. This time is also likely to vary depending on the scale of the system in question, in relation to the time it takes for storms to track over an entire catchment.

In our subsequent analysis, we considered only events with five or more active flumes (given our focus on large-scale connectivity), and for these events, rainfall and runoff measurements from across the entire watershed were

Table 1
Flume Features

Flume	East	North	Elevation	Contributing area (km^2)
1	580206	3510738	1,227	147.4268684
2	585357	3511395	1,292	111.5467424
3	589111	3511152	1,335	9.336293474
4	590422	3511788	1,359	2.257286909
6	589412	3510315	1,345	92.87341819
7	585334	3511251	1,298	13.98190881
9	592281	3509686	1,372	23.83398244
10	592400	3509923	1,372	15.64508555
11	595224	3512227	1,426	7.89603477
15	590945	3509061	1,355	23.28852903
102	589740	3512251	1,360	0.021010876
103	589541	3512372	1,362	0.036216116
104	589757	3512144	1,350	0.046629401
105	589521	3512390	1,361	0.002948895
106	589636	3512232	1,358	0.007095778
112	600058	3511785	1,513	0.019812888
113	599790	3511697	1,503	0.268994509
121	591321	3510937	1,359	0.055107474
125	589724	3510335	1,336	0.064967841

included in the analysis. This approach does nevertheless preclude analysis of the smallest, localized rainfall events. After the runoff data preprocessing, the time resolution of the hydrographs was kept at 1 min and the missing values of the raw data were filled with linear interpolation.

The rainfall data were filtered to retain measurements from rain gauges that lie within the watershed. To pair rainfall events with the runoff response at the watershed scale, rainfall data were selected such that there were no time gaps exceeding 1 hr between consecutive rainfall recordings when tracing backward in time from the onset of runoff and forward from the end of the runoff response. The time resolution for the rainfall timeseries was also kept at 1 min after the preprocessing. The intervening missing values were completed with the rainfall rate value from the previous time point. The last step in the data preprocessing for each rainfall event was to further filter for the measurements that were recorded only by the gauges located within the contributing areas of the watershed that drain into the flumes activated during the corresponding runoff responses.

Overall, 240 rainfall-runoff events were extracted from the rainfall and runoff records for the period spanning 2000 to 2024. Figure 2 illustrates the pipeline of our investigation and summaries of the runoff events and the rainfall event characteristics are provided in Tables S1 and S2 in Supporting Information S1.

2.3. Structural and Functional Connectivity

Our approach is centered upon a spatialized network-based analysis of connectivity. The watershed constitutes the boundaries of the system, and the structural river network comprises nodes - represented by the location of flumes–and links, formed either based on the hydrological pathways between

Table 2
Channel Features and Computations of the Flow River Network

Flume label (source)	Flume label (target)	Length (km)	Width (m)	Slope (m/m)	R_h (m)	V (m/s)	Time lag (min)
2	1	6,833	26	1.03	0.29	0.89	64
3	2	4,287	10	0.94	0.28	0.84	44
4	3	2,032	5	1.26	0.27	0.93	19
6	2	4,733	28	0.89	0.29	0.83	48
7	1	6,784	16	1.04	0.29	0.89	64
9	6	4,515	15	0.88	0.29	0.82	46
10	6	4,544	16	0.90	0.29	0.83	46
11	6	8,116	10	1.15	0.28	0.92	75
15	6	2,483	15	0.86	0.29	0.81	26
102	104	1.11	1	3.93	0.19	1.30	1
103	2	5,105	1	1.42	0.19	0.78	63
104	2	5,517	1	1.20	0.19	0.72	74
105	2	5,109	1	1.42	0.19	0.78	63
106	104	1.54	1	3.98	0.19	1.31	1
112	9	11,601	2	1.18	0.23	0.82	129
113	9	11,707	2	1.16	0.23	0.81	132
121	6	2,909	1	1.24	0.19	0.73	38
125	6	4.13	1	2.17	0.19	0.97	4

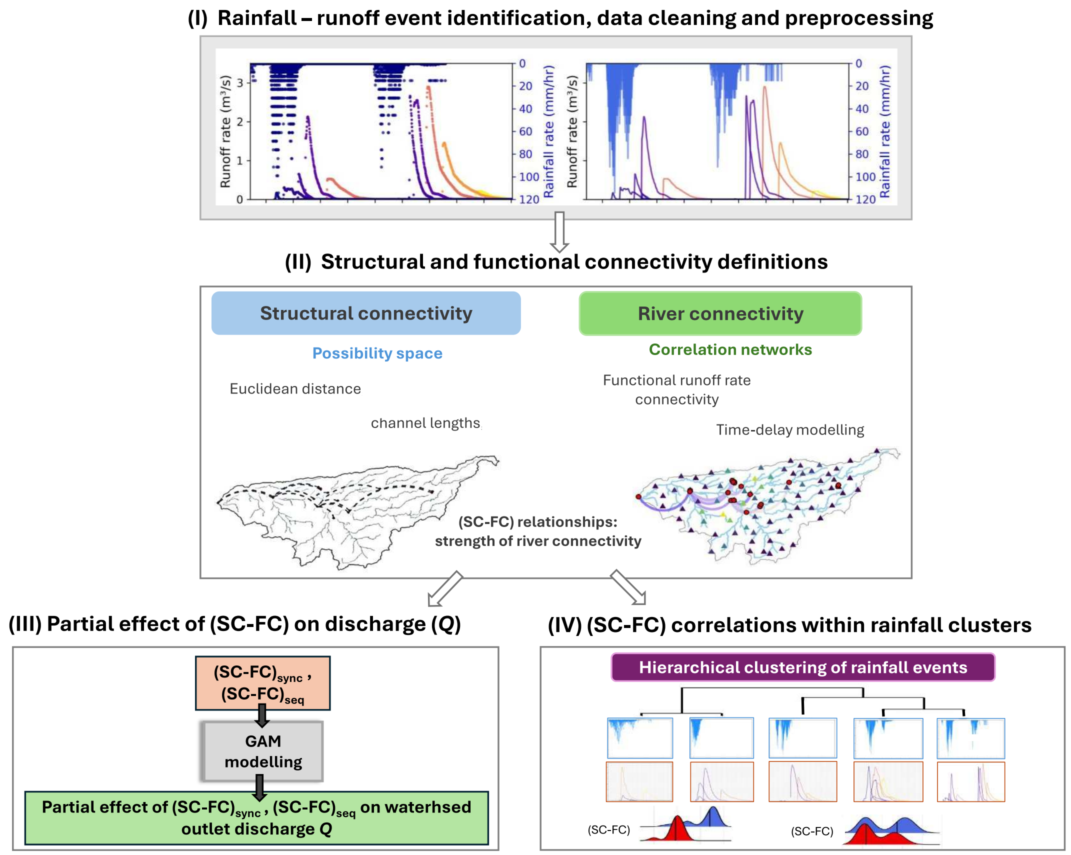

Figure 2. Schematic representation of our study: (I) Raw Walnut Gulch Experimental Watershed data enter a data cleaning, a subsequent event separation and a preprocessing pipeline. (II) Different versions of structural and functional connectivity defined and computed for each event. (III) Partial effects of $(SC - FC)_{sync}$ and $(SC - FC)_{seq}$ on discharge at the catchment outlet through Generalized Additive Model modeling. (IV) Categories of rainfall events extracted via hierarchical clustering and statistically compared with SC - FC correlations.

flumes (in the case of the sequential connectivity analysis) or other relational connections between them, such as spatial proximity (in the case of the synchronous connectivity analysis). These networks serve as templates where water flow and other processes occur. In line with previous studies (e.g., Deng et al., 2018; Woh, 2017), we are concerned with both functional and structural connectivity. We therefore define the network such that nodes are locations (i.e., flumes) with available discharge measurements, as our analysis is based upon characterizing the dynamics of the nodes. Hence, our network-construction approach differs from Tejedor et al. (2015) due to the fundamental difference in the data underpinning our functional connectivity analysis: they simulate fluxes through delta networks using the "package of flux" approach along network edges whereas we use discharge measurements at flumes. This difference—dynamical data at nodes compared to dynamical data along edges—is the reason behind our different approach to network construction. In addition, our analysis requires the same formalisation of the SC network as the FC network in order to calculate the SC - FC correlations.

Our conceptualization of the two distinct structural networks is based on the following rationale: synchronous connectivity results from simultaneous hydrological response, where the timing and shape of the runoff timeseries are consistent across multiple locations. Hence, flumes that are close in space (i.e., in adjacent sub-watersheds), but not necessarily located upslope/downslope can be simultaneously active. For this reason, the inverse Euclidean distance is an appropriate feature to be used in deriving the SC_{sync} network, as it draws stronger links between flumes that lie in closer proximity to one another, indicating the higher probability of synchronous activation. Figure 3a presents the network representation of SC_{sync} on the WGEW map, where the links denote the inverse of proximity between flumes, as defined by Equation 1a. Figure 3b shows the corresponding adjacency matrix of SC_{sync} derived from Equation 1a.

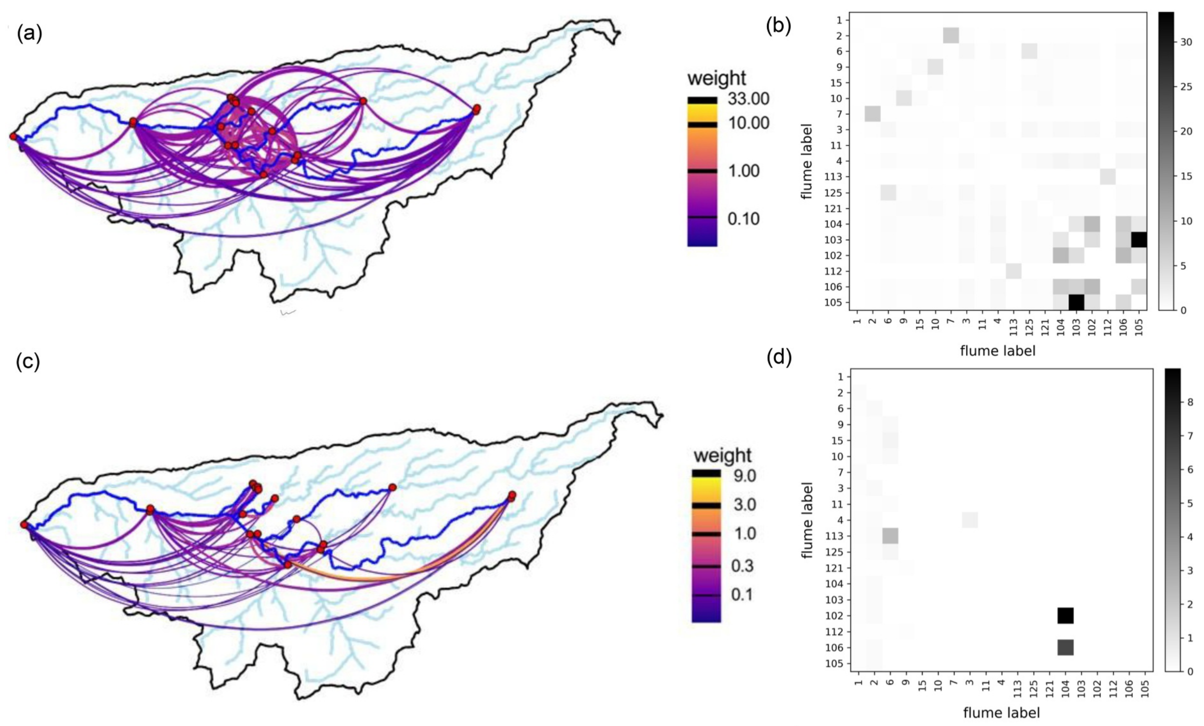

Figure 3. (a) Structural network with the links representing the spatial proximity between each pair of flumes. This structural template serves as possibility space that can capture the synchronous activation of flumes after precipitation. (b) The weighted adjacency matrix of the SC_{sync}. The weights result from the inverse Euclidean distance between each pair of flumes and the flumes are ordered by decreasing contributing area. (c) Structural network where the weighted links represent the inverse length of the hydrologically connected pathways. This structural template encompasses all possible paths where the flow of water can occur, hence it is suitable to capture the sequential activation of flumes. (d) The weighted adjacency matrix of SC_{seq}. The weights result from the inverse channel lengths and the flumes are ordered by decreasing contributing area.

Sequential connectivity on the other hand, reflects the connectivity shaped by water flowing through the river network. Thus, the length of the channels between the flumes is the key structural feature that affects how the water flows through this ephemeral system. Shorter channel lengths form stronger structural connections between the flumes. Figure 3c shows the weighted links between the flumes, as computed by the inverse channel length between each pair of flumes. Figure 3d depicts the corresponding sequential adjacency matrix, as defined in Equation 1b.

The weighted SC matrices are mathematically described as follows:

$$SC_{sync_{ij}} = \frac{1}{d_{ij}} \tag{1a}$$

$$SC_{seq_{ij}} = \frac{1}{l_{ij}} \tag{1b}$$

where d_{ij} is the Euclidean distance between flumes in km and l_{ij} is the channel length between flume i and flume j in km.

Functional connectivity (FC) can be represented as a matrix of pairwise correlations between hydrographs. Specifically, we calculated Pearson correlations between the runoff timeseries of the activated flumes during each event to capture linear similarities in the shape and phase of the runoff pulses. By computing correlations using both the original time series (to capture synchronous runoff responses) and time-shifted versions (to capture sequential dynamics), we can describe the overall connectivity characteristics of the river network in response to precipitation and the subsequent movement of water through the system with these two simple quantities. Network correlation approaches have been previously used in environmental sciences to establish statistical correlations between different locations and climate-topography interactions at continental and global scales (Peron et al., 2014).

The mathematical expression for the FC matrices is:

$$\mathrm{FC}_{sync_{ij}} = \mathrm{corr}_t(Q_i(t), Q_j(t)) \tag{2a}$$

$$\mathrm{FC}_{seq_{ij}} = \mathrm{corr}_t(Q_i(t), Q_j(t+\tau_{ij})) \tag{2b}$$

where $Q_i(t)$ is the time series of runoff rate at flume i within an individual event, τ_{ij} is the average time required for the water to reach flume j from flume i. To compute these times for each pair of flumes, we used the distance–time relation assuming a constant average flow velocity derived from Manning's equation:

$$V_{ij} = \frac{1}{n} R_h^{2/3} S_{ij}^{1/2}, \tag{3}$$

where V_{ij} is the cross-sectional average velocity between flumes i, j, R_h is the hydraulic radius, S is the slope of the stream and $n = 0.05$ is the Gauckler-Manning coefficient that accounts for the roughness. The hydraulic radius is given by the ratio $R_h = \frac{\text{cross-sectional area}}{\text{wetted perimeter}}$ and was calculated for average water depth of 0.5 m. Since the calculation of water velocities along each pathway between the flumes is based on channel characteristics (slope, roughness, geometry), the resulting time delays are values that primarily reflect the structural properties of the channel rather than event-specific dynamics, for example, relating to the transmission-loss process. This allows the usage of fixed, consistent time delay values between each pair of flumes $\tau_{ij} = \frac{l_{ij}}{V_{ij}}$ across all event cases, where l_{ij} is the channel length between flumes i, j. Table 2 provides a summary of all the above calculations.

SC - FC correlations were computed also as Pearson correlation between the SC_{sync}-FC_{sync} and SC_{seq}-FC_{seq} matrices, after excluding the diagonals and flattening the matrices, as a means of quantifying the degree of similarity between the structural and functional networks. The SC - FC correlation values were multiplied by a normalization factor, $N_f = \frac{\text{number of active flumes}}{\text{total number of flumes}}$, the number of active flumes corresponds to the number of flumes that recorded runoff during the event. The mathematical formula for the SC-FC relationships is the following:

$$\text{SC-FC} = N_f \, \mathrm{corr}_t(\mathrm{vec}_{\text{off-diag}}(\mathrm{SC}), \mathrm{vec}_{\text{off-diag}}(\mathrm{FC})) \tag{4}$$

Overall, the SC matrices we defined are mathematical representations of the river network that incorporate topographic features that facilitate either the synchronous activation of the flumes or the water flow along the river channels. The FC matrices are built as correlation networks of the runoff-rate timeseries and represent the hydrological connectivity in two forms, synchronous and sequential connectivity. In other words, FC describes how strongly different parts of the watershed respond simultaneously or with systematic time lag to the rainfall. Finally, the SC - FC relationships indicate how much the physical connections explain the functional similarity (runoff responses) and how strong each type of hydrological connectivity is. Table 3 summarizes the hydrological significance of the SC, FC and SC - FC relations.

2.4. Hydrologic Controls on SC-FC Relationships: Rainfall and Discharge

The first relations we looked for were between SC - FC correlations, rainfall amount and the accumulated runoff volume in flume 1, as a measure of the event size. The reason why we opted for flume 1 is because it optimizes the amount of data available for testing our approach. We computed the average rainfall across all raingauges to represent catchment-scale precipitation and along with the other variables we generated scatter plots to identify dominant trends among them.

To evaluate further dependencies between structural-functional connectivity metrics and the amount of discharge at the watershed outlet, we used Generalized Additive Models (GAMs). GAM analysis is often used in hydrology and geomorphology for rainfall - runoff modeling (Rashid & Beecham, 2019), streamflow prediction (Letcher et al., 2001), discharge modeling (Iddrisu et al., 2017) and regional estimation of low-flows and flood frequency at ungauged basins (Msilini et al., 2022; Ouarda et al., 2018). The approach is suitable as it can capture and model

Table 3
Description and Hydrological Significance of SC, FC and SC-FC Metrics

Connectivity metric	Concept	Hydrological significance
SC_{sync}	Characterizes the similarity of flumes, in terms of their spatial proximity	A higher SC_{ijsync} captures the higher potential for a synchronized response, based on structural catchment characteristics alone. Synchronized hydrological dynamics is likely to lead to an amplified hydrological response (see FC_{sync}).
SC_{seq}	Characterizes the spatial organisation of flumes within the dendritic network, the distance (along the river network) between flumes, with a time delay, informed by channel characteristics such as slope.	A higher SC_{ijseq} indicates a higher likelihood of a sequential (time delayed) hydrological response through flumes.
FC_{sync}	Quantifies the correlation of hydrographs of activated flumes during an event providing a measure of spatial extent and synchronicity of the runoff response.	The extent to which a runoff response in different locations within a catchment is co-activated. The downstream propagation of a synchronized flow response is likely to drive amplification of the flow response as well as hotspots of geomorphic change.
FC_{seq}	Quantifies the time-lagged correlation of hydrographs of activated flumes, and therefore provides a measure of flow connectivity between upstream and downstream locations within a river network.	Provides information on the extent to which different regions of a catchment contribute to an observed hydrological response at a catchment outlet, and therefore may provide insight as to the regions from which water and sediment (in the case of hotspots of geomorphic change) are transported to downstream locations.
$(SC-FC)_{sync}$	Quantifies how strongly the FC_{sync} response is controlled by the structural characteristics of the network.	This relation allows us to better understand how the realised synchronicity of the FC response in a rainfall-runoff event is related to the structural characteristics of the network. A comparison of this metric with $SC-FC_{seq}$ enables us to better understand the extent to which different types of runoff-inducing rainfall events lead to a synchronized response.
$(SC-FC)_{seq}$	Quantifies how strongly the FC_{seq} response is controlled by network characteristics (distance between flumes) versus dynamic properties of the storm event (rainfall characteristics, antecedent moisture, channel transmission losses).	The extent to which a connected downstream flow response is controlled by static properties of the network versus dynamic properties of the storm event (rainfall characteristics, antecedent moisture, channel transmission losses).

complex, nonlinear relationships between hydrological variables. Here, we tested both the additive and interactive effects of $(SC-FC)_{sync}$ and $(SC-FC)_{seq}$ on the accumulated runoff in flume 1. We applied an additive GAM, using the $(SC-FC)_{sync}$ and $(SC-FC)_{seq}$ values as predictors and the raw data from accumulated volume of runoff in flume 1 as the response variable. This method allowed us to separately examine the partial effects of each connectivity metric on the discharge in flume 1. Furthermore, we applied a tensor GAM to capture the combined nonlinear interactions between the predictors ($(SC-FC)_{sync}$, $(SC-FC)_{seq}$). To carry out these analyses the Python pyGAM library was used.

2.5. Classification of Rainfall Events

Hierarchical clustering is an unsupervised learning technique used approach to construct classification schemes that do not require the number of clusters to be predefined (Ran et al., 2023). Typically, hierarchical clustering is used when the quantities to be classified are characterized by a set of attributes, represented by numerical values. Here, we identified five key features of the rainfall events in order to apply hierarchical clustering on them: (a) number of rain gauges that are activated during the event, (b) the duration of the event, (c) the average rainfall intensity, (d) the maximum rainfall intensity within a time-window and (e) the Antecedent Dry Period (ADP) (number of days passed since the last rainfall). The exact values for rainfall characteristics across all rainfall events are given in Table S2 in Supporting Information S1.

The window within the rainfall intensity computed was selected based on the duration of the rainfall event, as follows: for events lasting 0–30 min: $\Delta t_{\text{window}} = 5$ min, 30–90 min: $\Delta t_{\text{window}} = 15$ min, 90–270 min: $\Delta t_{\text{window}} = 30$ min, 270–360 min: $\Delta t_{\text{window}} = 60$ min, 360–5000 min: $\Delta t_{\text{window}} = 120$ min. The calculations with respect to the ADP were based on aggregated daily data. A minimum threshold of 0.1 mm of average rainfall depth was used to classify a day as rainy. With regards to the rainfall intensity calculations only the raingauges

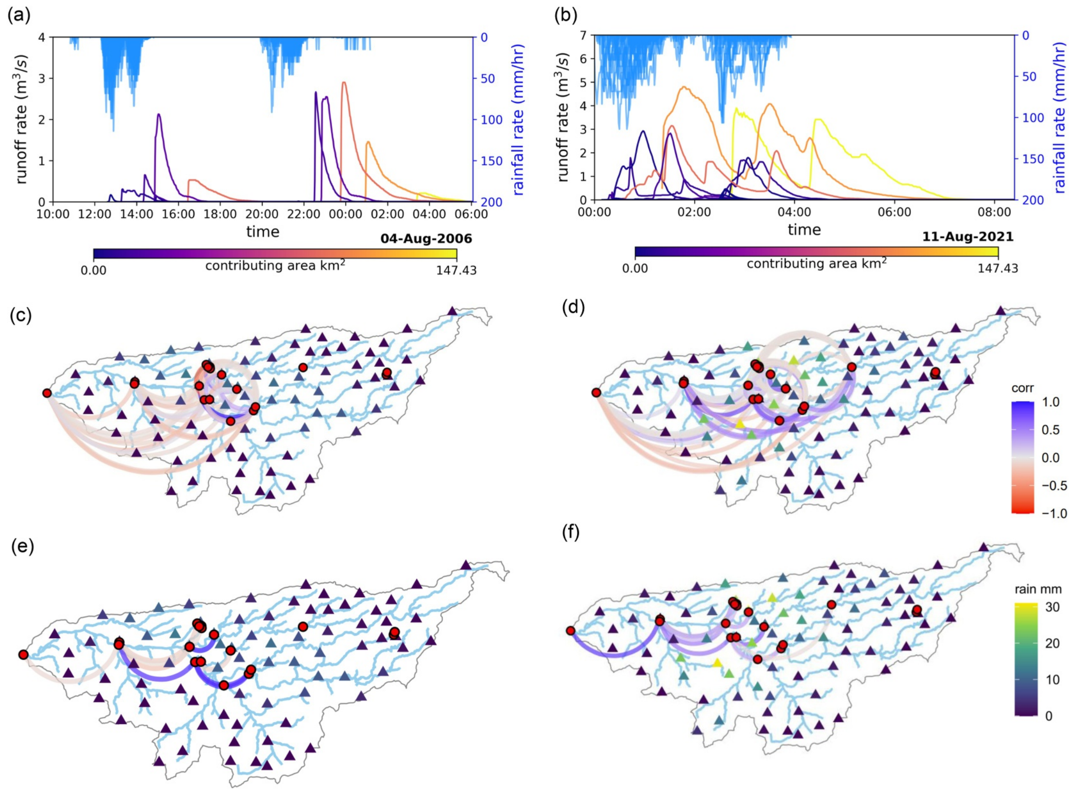

Figure 4. Representative examples of different hydrograph patterns and corresponding FC_{sync} and FC_{seq} networks on the Walnut Gulch Experimental Watershed map. (a) Hydrograph for event 45. The color of the runoff rate curves represents the size of the contributing area of the corresponding flume (gradual increase from dark to light colors), roughly indicating the downstream flow of the water. (b) Hydrograph for event 201. (c) FC_{sync} network for event 45. (d) FC_{sync} network for event 201. (e) FC_{seq} network for event 45. (f) FC_{seq} network for event 201.

that contribute into the flow of the activated flumes were taking into account. The rainfall feature values were normalized using the MinMaxScaler method from the scikit-learn library in Python before clustering. The dendrogram and clustering results were generated using functions from the SciPy library.

For each rainfall cluster, we used kernel density estimates (KDE plots) to visualize the total discharge through each flume activated during the events, in order to identify patterns and compare discharge distributions across flumes within each cluster. The analysis was performed using the ggplot2 library in R.

AI tools were used by some authors to assist with language editing and text clarification.

3. Results

3.1. Structural–Functional Connectivity Relations

First, we present a visualization of functional connectivity for two contrasting events at the WGEW (Figure 4). The first event occurred on 3rd–4th August 2006 (event 45), with an average rainfall depth of 9.5 mm, and a watershed-scale runoff coefficient of 0.0006. The second event occurred on 11th August 2021 (event 201), with an average rainfall depth of 6.7 mm, and a watershed-scale runoff coefficient of 0.026. Hence, they are relatively similar in terms of their overall rainfall amount, but vary considerably in terms of the timing and spatial distribution of rainfall, the number of flumes activated and the magnitude of flow. The functional connections between the flumes can be either positive, indicating a high degree of synchronicity in the runoff pulses, or negative, indicating that the runoff pulses are out of phase.

Both values of $(SC\text{-}FC)_{sync}$ and $(SC\text{-}FC)_{seq}$ for event 45 are close to zero ($(SC\text{-}FC)_{sync} = 0.04$ and $(SC\text{-}FC)_{seq} = 0.0097$, see Figure 5), which is indicative of the very weak overall connectivity across the

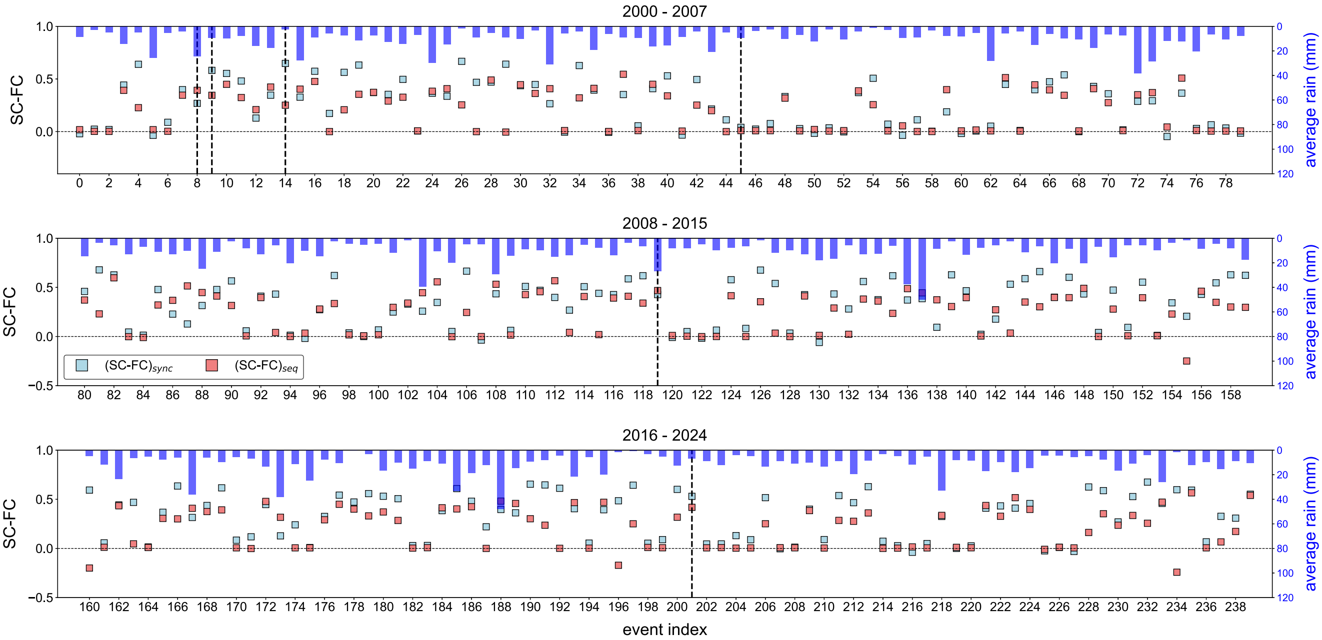

Figure 5. SC-FC correlations across the years 2000–2024 for runoff events, in which five or more flumes were activated. The blue bars indicate the total rainfall depth at the end of the event. The vertical black dashed lines indicate the SC - FC correlation for the events whose FC matrices are shown in Figures 4 and 6.

watershed. In event 201, the overall connectivity exhibits almost opposite behavior. Both $(SC - FC)_{sync}$ and $(SC - FC)_{seq}$ are relatively high, ($(SC - FC)_{sync} = 0.53$ and $(SC - FC)_{seq} = 0.42$, see Figure 5), indicating that the watershed is adequately hydrologically connected in terms of both synchronous and sequential activity.

These two events are illustrative of the high variability in $(SC - FC)_{sync}$ and $(SC - FC)_{seq}$ values computed for each event over the 24-year period (Figure 5). From a visual inspection of the scatter plot (Figure 5), we observe that the events, described by the two correlation values, can be divided into four groups: (a) events that favor equally synchronous and sequential connectivity, (b) events dominated by synchronous connectivity, (c) events where sequential connectivity is more pronounced, and (d) events where the functional connectivity is poorly correlated with the underlying SC.

3.2. Interplay Between $(SC - FC)_{seq}$ and $(SC - FC)_{sync}$

Figure 6 shows representative examples of hyetographs-hydrographs during rainfall - runoff events, their corresponding patterns of FC_{sync} and FC_{seq}, along with the SC - FC correlations and the accumulated volume of water in flume 1. In Figure 6a we can see a typical example of water-flow process (event 8), in which the runoff originates at the more upstream flumes and gradually propagates downstream. A substantial area of the catchment is covered by water flow, thus FC_{seq} spans a significant portion of the possibility space, resulting in a moderate $(SC - FC)_{seq}$ value (0.39). Transmission losses during this event appear to be small, as indicated by the large water accumulation in flume 1, at the watershed outlet. Figure 6b illustrates an event with two distinct activity peaks in the upstream areas (event 9). The synchronous activation of flumes is mainly confined to these upstream zones, where flumes are located in close proximity and correspond to relatively small contributing areas ($\approx$0.035 km^2). Highly correlated flow activity occurs between flumes 104 and 106, and between 104 and 102 during both phases of the event. Only the water flow from phase 1 reaches flume 1. The pronounced functional connections in this event are reflected by the relatively high correlation values ($(SC - FC)_{sync} = 0.58$, $(SC - FC)_{seq} = 0.34$).

In Figure 6e, we see an example of hydrograph patterns that appears frequently among the runoff events identified in the data (event 14). It is one of the cases in which the flow response in flumes 102, 103, 104, 105 and 106 exhibits a high degree of synchronization, evidenced by a notably high $(SC - FC)_{sync}$ correlation (0.65), partly driven by the high density of sensors in this localized subarea. The rainfall and runoff amounts for this event are low, and the synchronized response of the activated flumes did not propagate to downstream locations. The event

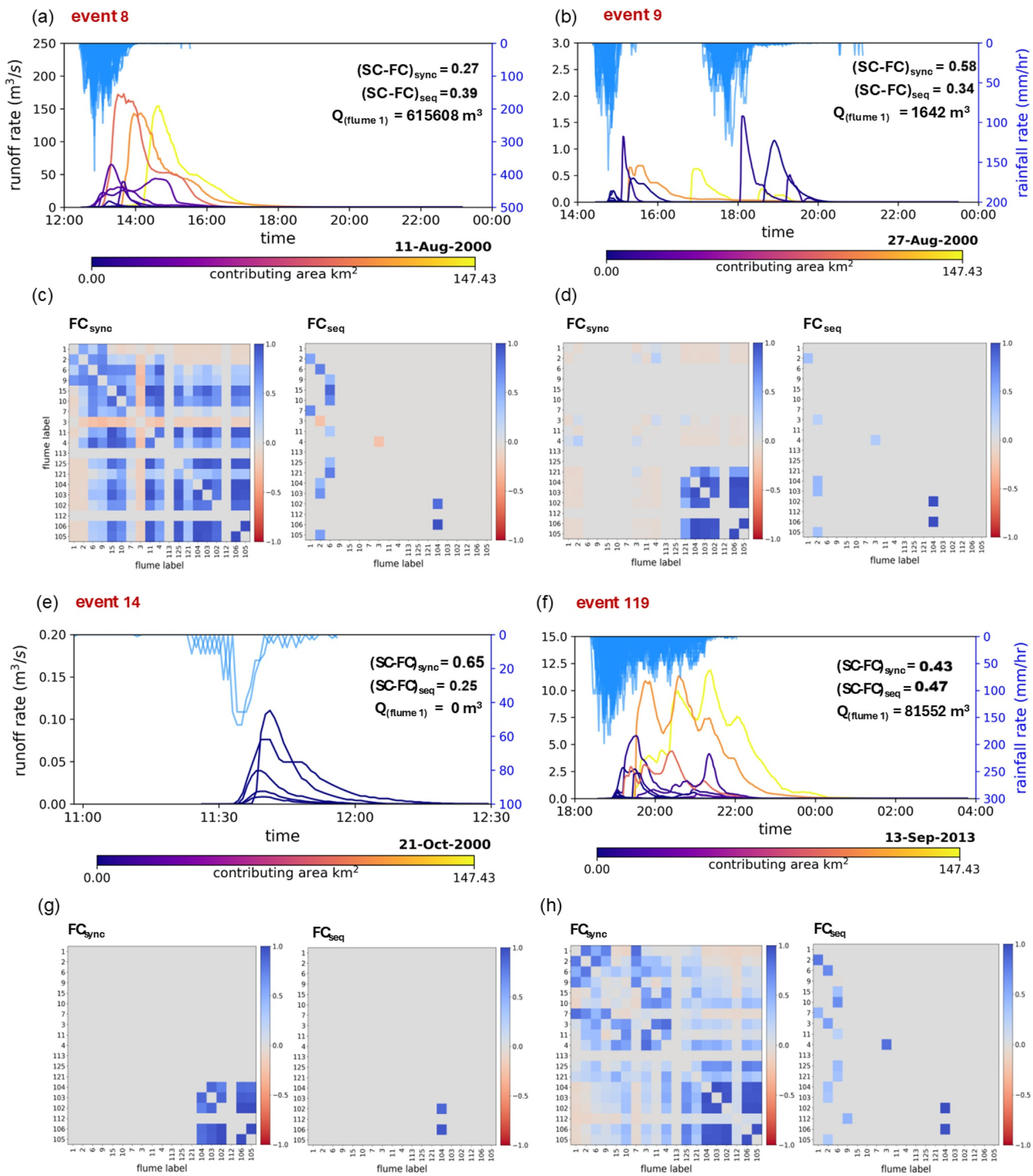

Figure 6. (a, b) and (e, f): Hydrographs–hyetographs of selected events illustrating different rainfall pattern–runoff responses. Above each event plot, the SC - FC correlation and the accumulated water volume in flume 1 are given. (c, d) and (g, h): FC matrices, SC - FC correlations and accumulated discharge at flume 1 corresponding to the selected events. In the FC matrices, flumes are ordered by contributing area. The FC matrices represent the connectivity patterns. In the subsequent clustering analysis, event 8, 9, 119 belong to cluster 4 and event 14 to cluster 1.

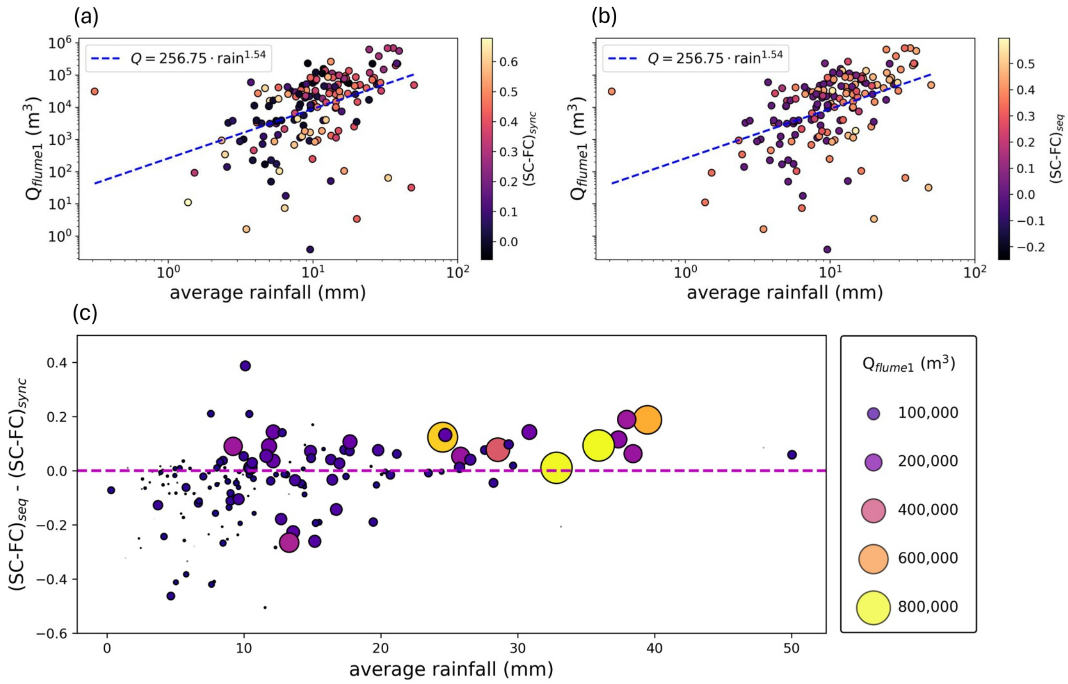

Figure 7. (a) Scatter plot of average rainfall depth across the watershed versus accumulated volume at Flume 1. Color shading indicates $(\mathrm{SC}-\mathrm{FC})_{sync}$ correlation values. (b) Scatter plot of average rainfall depth across the watershed versus accumulated volume at Flume 1 (Q). Color shading indicates $(\mathrm{SC}-\mathrm{FC})_{seq}$ correlation values. (c) Scatter plot of average rainfall depth across the watershed versus the difference $(\mathrm{SC}-\mathrm{FC})_{seq} - (\mathrm{SC}-\mathrm{FC})_{sync}$. Color shading and the size of the markers indicate the size of the events based on Q.

at Figure 6f, shows the event 119, which is characterized by higher $(\mathrm{SC}-\mathrm{FC})_{seq}$ correlation value (0.47). During event 119, 18 out of 19 flumes were activated and this widespread flume activation contributes to the increased SC - FC correlation values.

Figure 7 illustrates the relations among rainfall depth, runoff event size—described by the accumulated water volume at flume 1—and the SC - FC correlations. In Figure 7a, we can observe that events with higher $(\mathrm{SC}-\mathrm{FC})_{sync}$ values often correspond to cases where at least one of the two hydrological variables (rainfall depth or Q) is of small or moderate magnitude. Figure 7b illustrates that there is a larger variability in the values of rainfall depth or Q that are related to high $(\mathrm{SC}-\mathrm{FC})_{seq}$ values (light colors), with events characterized by larger rainfall and runoff volumes to typically display higher correlation values. Finally, Figure 7c focuses on the interplay between $(\mathrm{SC}-\mathrm{FC})_{sync}$ and $(\mathrm{SC}-\mathrm{FC})_{seq}$, expressed as the difference between these two metrics. In other words, it demonstrates the relative strength of $(\mathrm{SC}-\mathrm{FC})_{seq}$ compared to $(\mathrm{SC}-\mathrm{FC})_{sync}$. We can observe that the largest events cluster around positive differences and higher average rainfall amounts, implying that stronger $(\mathrm{SC}-\mathrm{FC})_{seq}$ translates to sustained connected flow across the watershed. At lower rainfall amounts the differences are more variable, with a tendency of smaller events to show significantly higher $(\mathrm{SC}-\mathrm{FC})_{sync}$ than $(\mathrm{SC}-\mathrm{FC})_{seq}$.

For a more detailed analysis of the relations between SC - FC correlations as metrics of the runoff connectivity and the discharge at the watershed's outlet $\left(Q_{\mathrm{flume1}}\right)$, we used two Generalized Additive Models (GAM). The fitted models revealed how individual and joint variations in $(\mathrm{SC}-\mathrm{FC})_{sync}$ and $(\mathrm{SC}-\mathrm{FC})_{seq}$ shape and influence the runoff magnitude. Figure 8 shows the partial dependence plots from the additive GAM and the 95% confidence interval (Figures 8a and 8b), namely the marginal contribution of each individual predictor. In particular, the partial effect of $(\mathrm{SC}-\mathrm{FC})_{sync}$ on Q_{flume1} exhibits small positive values at lower correlations, a local peak at intermediate correlations followed by a dip, as the values increase. This suggests that events with small or moderate accumulated volume Q_{flume1}, tend to have small $(\mathrm{SC}-\mathrm{FC})_{sync}$ values (<0.3), the larger events are typically characterized by intermediate $(\mathrm{SC}-\mathrm{FC})_{sync}$ values (≈0.3), whereas events with low or zero water accumulation in the outlet exhibit small negative $(\mathrm{SC}-\mathrm{FC})_{sync}$ values. The effect of $(\mathrm{SC}-\mathrm{FC})_{seq}$ on Q_{flume1} shows a smoother

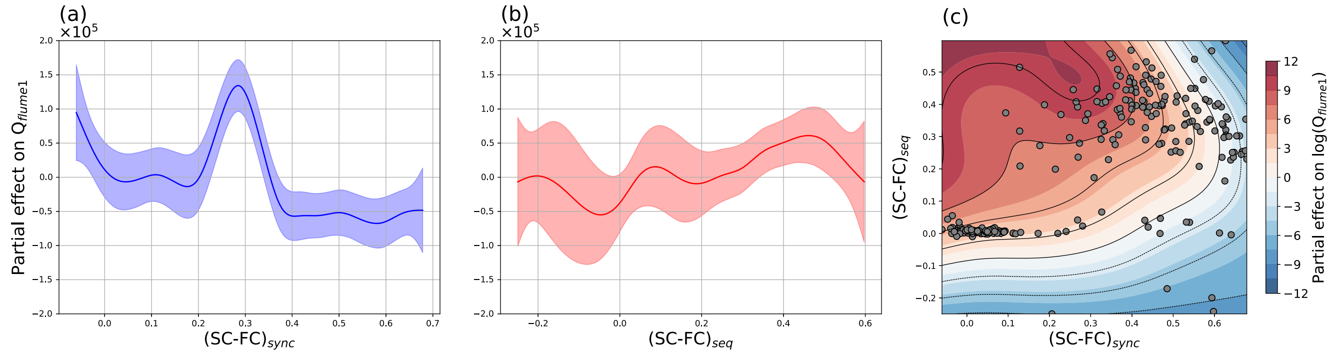

Figure 8. (a) Partial effect of $(\mathrm{SC-FC})_{sync}$ on the response variable Q_{flume1}, showing the estimated smooth relationship while holding $(\mathrm{SC-FC})_{seq}$ constant at its mean. (b) Partial effect of $(\mathrm{SC-FC})_{seq}$ on the response variable Q_{flume1}, showing the estimated smooth relationship while holding $(\mathrm{SC-FC})_{sync}$ constant at its mean. (c) Interaction effect between $(\mathrm{SC-FC})_{seq}$ and $(\mathrm{SC-FC})_{sync}$ on the response variable Q_{flume1} as modeled by the tensor product smooth. Color contours represent the magnitude and direction of the combined effect, with black contour lines for clarity. Data points are shown in gray.

increasing trend across the increasing correlation range. In Figure 8b we observe that Q_{flume1} exhibits a slight, overall increasing tendency. The negative $\mathrm{SC-FC}_{seq}$ values indicate events with high variability at their sizes and the peak is reached at $(\mathrm{SC-FC})_{seq} = 0.41$. Further increase indicates lower values for Q_{flume1}. The model explained 28.9% of the deviance (pseudo $R^2 = 0.289$) and had an AIC of 6121.5819 and with a GCV score of 7.3×10^9. Both predictors showed significant nonlinear effects on runoff ($(\mathrm{SC-FC})_{sync}$: edf (effective degrees of freedom) = 7.5, $p < 0.001$, $(\mathrm{SC-FC})_{seq}$: edf = 6.3, $p < 0.001$).

The contour plot shown in Figure 8c depicts the output of the tensor GAM and highlights the combined nonlinear interactions between the predictors ($(\mathrm{SC-FC})_{sync}$, $(\mathrm{SC-FC})_{seq}$). The tensor-product GAM was applied to the log-transformed discharge data in flume 1. Zero values were handled by substituting a small constant (10^{-3}) prior to log transformation. The general trends of how the $(\mathrm{SC-FC})_{sync}$ and $(\mathrm{SC-FC})_{seq}$ follow those described by the partial effects and no strong nonlinear interaction between the two predictors is observed. This model gave a pseudo R^2 of 0.29 and edf of 12.4, with a significant interaction effect between the two predictors ($p < 0.001$). The AIC was slightly lower (6119.5) compared to the additive GAM model and the GCV slightly lower, too (7.2×10^9).

Furthermore, Figure 3c indicates a threshold effect in $(\mathrm{SC-FC})_{sync}$ that must be reached before $(\mathrm{SC-FC})_{seq}$ becomes positive. Specifically, positive values of $(\mathrm{SC-FC})_{seq}$ appear only when $(\mathrm{SC-FC})_{sync} > 0.13$. This finding supports further the argument that localized synchronous activity must precede watershed-scale propagation, hence leading to sequential activity.

3.3. Rainfall–Runoff Clusters

We used hierarchical clustering to investigate the event rainfall data at various levels of similarity in feature space. The final clustering revealed four distinct rainfall groups, identified as the optimal number of clusters based on silhouette scores and Wilks' lambda calculated across various clusterings. It should be noted that there is no inherent relationship between the two types of event classification (rainfall clustering and classification based on the connectivity values), they are rather independent. The first is based purely on observations of the pairs of SC - FC values, while the second arises from mapping the SC - FC correlations onto the rainfall groups identified through hierarchical clustering. However, this rough similarity may indicate an intrinsic relationship between rainfall characteristics and the resulting SC - FC signatures.

Figure 9a shows the heatmap and the dendrogram of the normalized rainfall features and Figure 9b the corresponding boxplots of three scaled rainfall characteristics (number of gauges, duration, average intensity). We performed Multivariate Analysis of Variance (MANOVA) to assess the significance of differences across the clusters. The MANOVA results yielded Wilks' lambda = 0.0195, with an associated p-value <0.001, indicating highly significant and substantial differences in the multivariate profiles across clusters. Cluster 1 includes localized events with high intensity and short duration. The median value of its distribution of the number of

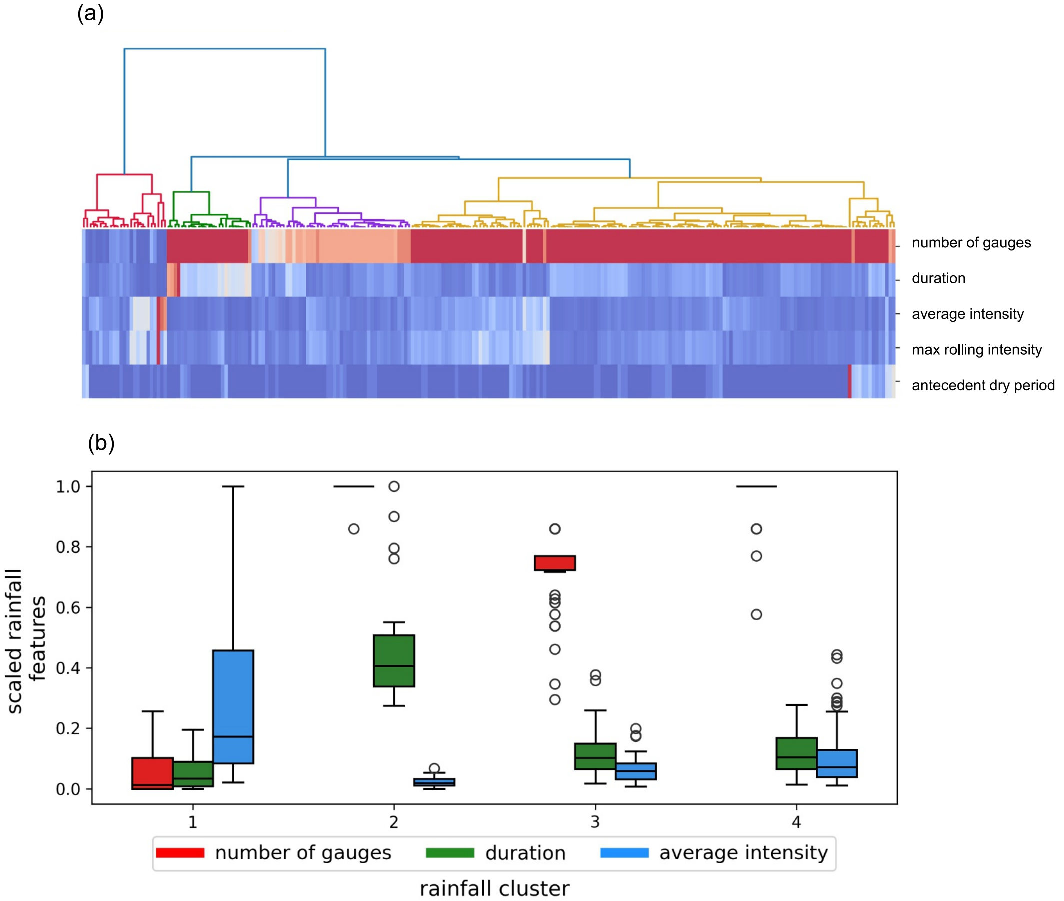

Figure 9. (a) Heatmap and dendrogram of rainfall features (b) boxplots of the scaled rainfall features within the clusters. MAVONA results on the scaled rainfall features yielded Wilks' lambda = 0.0195, with an associated p-value <0.0001, which suggests strong and statistically significant differentiation of the medians across the clusters.

active gauges is 4, the median of the average intensity is 6.1 mm/hr and the median of duration is 1.3 hr. The events that comprise cluster 2 are spatially uniform and have low intensity and long duration. The median values are 81 for the number of gauges, 0.85 mm/hr for the average intensity, and 13.7 hr for the duration. The rainfall events in cluster 3 exhibit moderate spatial coverage (the median value for the number of active gauges is 63), moderate average intensity (median = 3.3 mm/hr) and medium duration (median = 3.6 hr). Finally, cluster 4 includes events spatially extended (the median value for the number of active gauges is 81), whereas the average intensity and duration are also moderate (median values 2.6 mm/hr and 3.7 hr, respectively).

Figures 10a and 10b show the scatter plots and boxplots of the $(SC\text{-}FC)_{sync}$ and $(SC\text{-}FC)_{seq}$ across the clusters identified based on the rainfall characteristics. We also performed MANOVA to compute Wilks' lambda along with the p-value on the SC-FC clusters. The output in this case showed weaker groups differences (Wilks' lambda = 0.7112), with statistical significance, though (p-value <0.0001). Cluster 1 is characterized by clear dominance of $(SC\text{-}FC)_{sync}$ (median = 0.6) over $(SC\text{-}FC)_{seq}$ (median = 0.26), whereas cluster 2 exhibits slight preference towards $(SC\text{-}FC)_{seq}$ $(\text{med}((SC\text{-}FC)_{sync}) = 0.25, \text{med}((SC\text{-}FC)_{seq}) = 0.3)$. In cluster 3, despite the overlap between the $(SC\text{-}FC)_{sync}$ and $(SC\text{-}FC)_{seq}$ distributions, there is a significant difference in their median values, with $(SC\text{-}FC)_{sync}$ showing a higher median (0.43) compared to $(SC\text{-}FC)_{seq}$ (0.01). Finally, in cluster 4 the median values of the two types of SC-FC $(\text{med}(SC\text{-}FC)_{sync} = 0.36, \text{med}(SC\text{-}FC)_{seq} = 0.29)$, which suggests comparable overall importance of the two FC types in the cluster.

Figure 11 shows the density plots for the accumulated runoff per cluster along with the density distributions of SC-FC correlations. In cluster 1 (25 flow events), the flumes with larger contributing areas (>15 km^2) are not

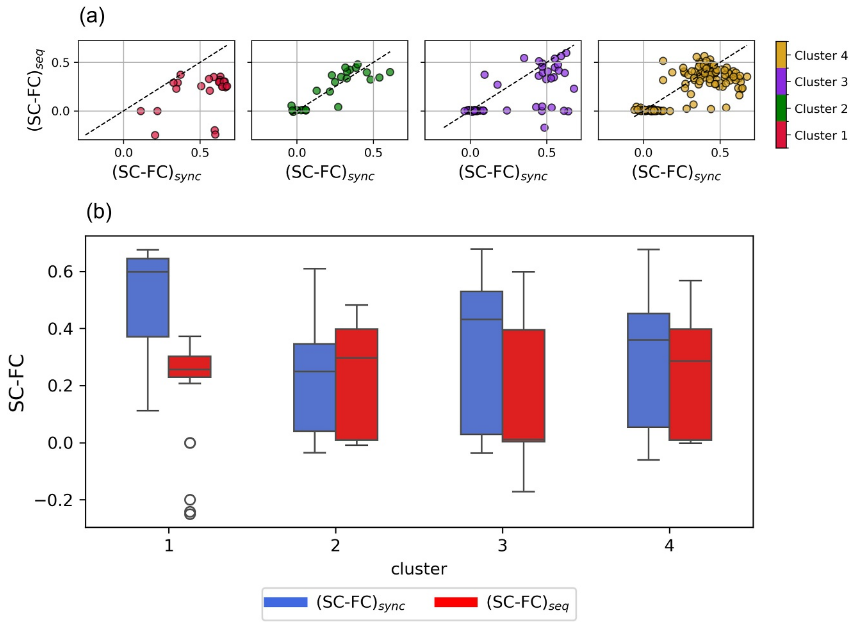

Figure 10. (a) Scatter plots of $(SC\text{-}FC)_{sync}$–$(SC\text{-}FC)_{seq}$ within the clusters (b) Boxplots of $(SC\text{-}FC)_{sync}$ and $(SC\text{-}FC)_{seq}$ within the clusters. Multivariate Analysis of Variance results gave Wilks' lambda = 0.7112, which indicates weaker group differences and moderate multivariate effect. The low p-value <0.0001 indicates that these weak differences are highly statistically significant.

activated. Hence, it can be inferred that the synchronous and sequential flow connectivity is occurring in the mid to upper reaches of the watershed. Flume 103 was activated during all 25 flow events in this cluster, whereas flume 10 was only activated during 2 flow events. These events are characterized by high $(SC\text{-}FC)_{sync}$ (median = 0.6) and moderate $(SC\text{-}FC)_{seq}$ (median = 0.26). In cluster 2, SC-FC values are wide-ranging. The median of $(SC\text{-}FC)_{seq}$ is 0.3 and exceeds the median value for the $(SC\text{-}FC)_{sync}$ (0.25). Of the 25 events in this cluster, all but 1 generated flow that reached the watershed outlet, although only three of these events had an increase in flow from flume 2 and 1. In cluster 3, both SC-FC density distributions have bimodal peaks, but with contrasting median values, of 0.43 for $(SC\text{-}FC)_{sync}$ and 0.01 for $(SC\text{-}FC)_{seq}$. Of the 47 events in this cluster, none of them generated flow that reached the watershed outlet. Flow discharge decreased in the main channel, between flumes 6 to 2, and infiltrated between flumes 2 and 1 during 34 events.

The widespread, shorter duration, and higher intensity rainfall events in cluster 4 ($n = 143$) led to a wide-ranging runoff response and SC-FC values, with 138 of these events generating flow that reached the watershed outlet. The median value for the $(SC\text{-}FC)_{sync}$ is 0.36 and the median for the $(SC\text{-}FC)_{seq}$ is 0.29.

4. Discussion

4.1. Event-Scale SC-FC Correlations and the Interplay Between $(SC\text{-}FC)_{sync}$ and $(SC\text{-}FC)_{seq}$

In this study we have focused on the effects of rainfall characteristics on hydrological connectivity. The detailed analysis of FC_{seq} and FC_{sync}, and their respective SC-FC correlations, clearly show that these connectivity metrics along with traditional hydrological indicators reveal dominant relations between rainfall-runoff events. While water volume at the watershed outlet and peak discharge provide information about the event's magnitude and total runoff, these measures alone do not convey information about the underlying hydrological dynamics or the spatial distribution of the event. In contrast, SC-FC relations offer a more precise depiction of these spatial and structural characteristics. Therefore, a combination of both types of metrics yields a more comprehensive understanding of the event conditions and the overall system response, resulting in a more detailed and accurate interpretation of the occurring hydrological processes.

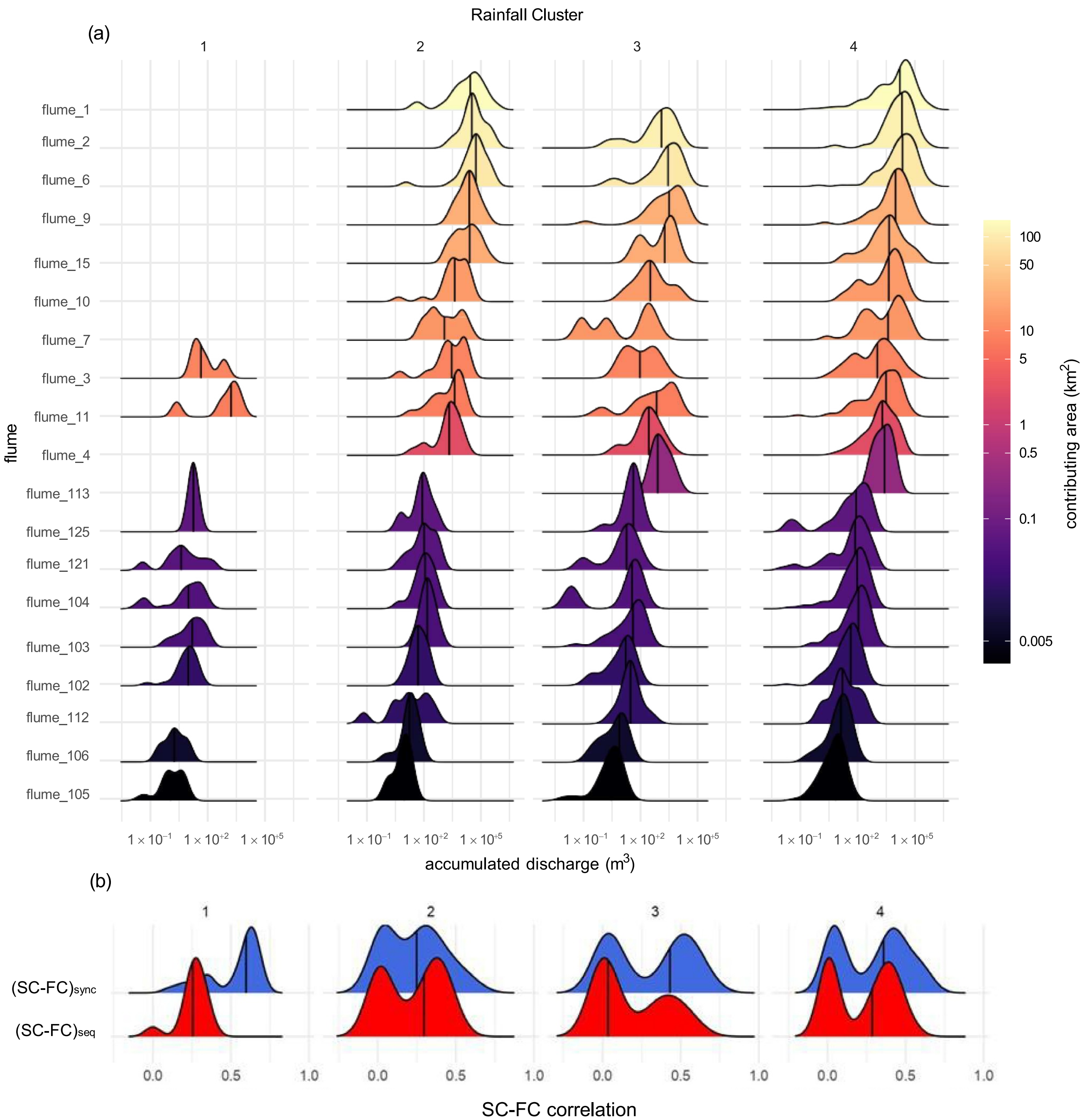

Figure 11. (a) Density plots for the total discharge passing through each flume across all events. Each row represents a rainfall cluster and the flumes are ordered with decreasing contributing area. This representation provides an approximate visualization of water flow across the watershed (from bottom to top). (b) Density plots of the SC - FC correlations for each corresponding event cluster.

In our case study, $(SC - FC)_{sync}$ correlations range between −0.06 and 0.68, whereas $(SC - FC)_{seq}$ correlations fall between −0.25 and 0.6. Events with high magnitude hydrological responses (indicated by the amount of discharge in flume 1) are typically described by high values of $(SC - FC)_{seq}$ (usually above 0.5) and moderate correlations for $(SC - FC)_{sync}$ (usually around 0.3), as Figures 7 and 8 show. This combination of values for the two types of connectivity is indicative of the importance for gaining insights about the overall hydrological response of the system. High $(SC - FC)_{seq}$ correlation values require spatially extended runoff events, with low transmission losses. On the other hand, $(SC - FC)_{sync}$ is more sensitive in capturing localized, very small events, often with non-significant hydrological response. The instrumentation of the watershed is a key factor that influences the SC - FC correlation values. Regions with dense structural connectivity favor the emergence of simultaneous activity in the FC and capture the synchronized small runoff patterns. For instance, areas with denser monitoring coverage—for example, strong hydraulic links between flumes 104 and 102, or 104 and 106—favor disproportionately $(SC - FC)_{sync}$, while less densely instrumented regions contribute to a loss of information regarding runoff dynamics. For example, flumes 9, 6, 2 and 1 are typically produce very clear and strong sequential runoff patterns, which (if the only ones) are undervalued in the SC - FC computation, as structural connectivity between them is relatively weak. This highlights a case where structural connectivity alone fails to adequately predict functional dynamics.

The largest hydrological events are characterized by the highest runoff rates and sharp discharge peaks, with minimal fluctuations in between. During these events, the rapid movement of water allows little time for infiltration, resulting in lower transmission losses and consequently higher discharge. These events typically exhibit strong functional connections or even flooding within the catchment, which may translate to reduced similarity to the weaker structural links. In contrast, events with the highest $(SC - FC)_{seq}$ values tend to have lower runoff rates and the hydrographs include noticeable fluctuations during the event. The variability in the runoff rates suggest larger diversity in the catchment responses and the longer travel times. These can lead to functional connections that are more similar to the structural ones and greater transmission losses, hence lower or no discharge at the watershed's outlet.

Pertinent questions remain surrounding the effects of the different rainfall characteristics and types of connectivity on the geomorphic response of these systems, especially given the episodic and spatially variable nature of geomorphic adjustments that characterize these systems (Bull, 1997; Hooke, 2016). The high variability of $(SC - FC)_{sync}$ with the rainfall-runoff response (Figure 7) may be attributed to the fact that $(SC - FC)_{sync}$ captures simpler hydrological responses between flumes. For instance, short and intense rainfall events can trigger simultaneous activation of flumes, particularly in densely instrumented subcatchments, without necessarily producing substantial flow across the entire watershed. The relationship between heavy precipitation in combination with high antecedent soil moisture has also been detected across larger landscapes, for example, in synchronicity of river flooding across Europe (Berghuijs & Kirchner, 2020). It has also been reported that the flood synchrony scale showed an increase during the past years (Berghuijs et al., 2019).

Rainfall events with a larger footprint typically have a lower rainfall intensity, and generate runoff responses that sustain water flow across the catchment for a longer time compared to short, intense localized events that produce synchronous runoff pulses. The sequential nature of the runoff pulses in the case of larger events contributes to large $(SC - FC)_{seq}$ values and medium $(SC - FC)_{sync}$ values. So we see that for the largest events a synchronous response observed over smaller spatial scales is a contributing factor to large SC/FC_{seq}, and thus both types of connectivity play a role in driving event magnitude. This coexistence of primarily sequential and partially synchronous behaviors is also supported by analyses of flood-generating processes (Merz & Blöschl, 2003).

Our connectivity measures provide an overall indication of the prevalence of the two types of connectivity within the watershed, regardless of whether or not flow is connected to the catchment outlet, as in the approach of Phillips et al. (2011) and Spence and Phillips (2015). Our results have demonstrated that highly connected flow, for either or both of $(SC - FC)_{sync}$ and $(SC - FC)_{seq}$ does not always lead to flow at the watershed outlet (flume 1), due to infiltration into the channel bed. Nevertheless, the prevalence of flow connectivity at locations within the watershed is still important in terms of in-channel processes such as local regions of erosion and deposition, redistribution of water within the watershed, and ecological and biochemical processes within the vegetated beads (Wainwright et al., 2002). In particular, events where connected flow does not reach the watershed outlet play an important role in determining the antecedent conditions for successive events (occurring within a short period of time), where transmission losses are likely to be reduced, and thus connectivity to the watershed outlet is likely to be maximized.

Some representative examples that support this statement are the events of 7th and 9th July 2013. During the initial event on 7th July, a moderate rainfall event was recorded (average rainfall = 9.55 mm). Despite the relative high connectivity ($(SC - FC)_{sync} = 0.47$, $(SC - FC)_{seq} = 0.46$), water flow did not reach flume 1. However, this suggests that the event primarily resulted in partial wetting of the channel network and saturation of the soil. Two days later, on July 9th, a subsequent rainfall event with a higher average rainfall of 15.03 mm generated sufficient runoff to produce connected flow across the system ($(SC - FC)_{sync} = 0.4$, $(SC - FC)_{seq} = 0.57$), and substantial amount of discharge reached at the watershed outlet (Q = 1846.54 m^3). Another example is the event that occurred on 1 July 2016. This event involved a moderate average rainfall of 20.33 mm, producing a substantial discharge at the outlet (Q= 14540.7 m^3) with connectivity values of $(SC - FC)_{sync} = 0.4$ and $(SC - FC)_{seq} = 0.39$. The day before, 30th June, there was a relatively small rainfall event (average rainfall = 6.5 mm), that produced runoff in some of the smaller tributaries of the river network ($(SC - FC)_{sync} = 0.66$, $(SC - FC)_{seq} = 0.3$). During this event, water flow did not reach flume 1, however it is likely that contributed to increased soil moisture that enhanced flow connectivity during the following day's event. There are also cases where multiple events happened within the same day; for instance, on 12 September 2016, event 156 with relatively low average rainfall (8.27 mm) generated large discharge at the catchment outlet (Q= 33895.27 m^3), along with high sequential connectivity ($(SC - FC)_{sync} = 0.43$, $(SC - FC)_{seq} = 0.46$). This enhanced response is very likely attributable to two smaller rainfall events earlier that same day, which prewetted different areas of the catchment. The resulting antecedent moisture conditions reduced infiltration losses and facilitated more efficient surface flow during the later event. The proximity of these events in time suggests that the antecedent conditions established by the former event played a critical role in reducing transmission losses during the latter, thus enhancing hydrological connectivity and facilitating water flow. These examples support the argument that events with zero outlet response can significantly influence the catchment's hydrologic connectivity and increase the discharge during subsequent runoff events.

The connectivity values refer to the specific study area, however the methodology can applied in the same way to larger watersheds. In larger catchments, storms moving across them can significantly influence the timing and pattern of the hydrological response. As rainfall moves across the basin, different sub-catchments contribute runoff at different times resulting in hydrographs with irregular form, compared to smaller catchments where the response is typically sharper and more predictable. Multiple peaks or delayed peak discharge may occur in these cases due to the spatial variability and nested structure of the larger catchments.

The relative consistency in the results between the two Generalized Additive Models, that is, between the interactive effect of $(SC - FC)_{sync}$ and $(SC - FC)_{seq}$ on Q_{flume1} with the partial effects indicates that the influence of the two connectivity metrics on the discharge is mostly independent and additive across the observed range.

The additive GAM explained 28.9% of the deviance in runoff and indicated significant nonlinear effects of both predictors ($(SC - FC)_{sync}$: edf = 7.5, $p < 0.001$; $(SC - FC)_{seq}$: edf = 6.3, $p < 0.001$). These effective degrees of freedom suggest moderately complex nonlinear relationships between each predictor and runoff.

The tensor-product GAM, which allows for interactions between the two connectivity metrics, produced a slightly improved model fit (pseudo $R^2 = 0.29$; AIC = 6119.5; GCV = 7.2×10^9) compared to the additive model (AIC = 6121.6; GCV = 7.3×10^9). The interaction between the two predictors was highly significant ($p < 0.001$), indicating that the influence of one predictor on runoff depends on the value of the other predictor.

However, the improvement in model performance was relatively small, suggesting that most of the explained variation in runoff is captured by the individual nonlinear effects of the connectivity metrics. Nevertheless, the tensor model provides additional insight into the joint influence of the $(SC - FC)_{sync}$, $(SC - FC)_{seq}$ and therefore represents a slightly better description of the underlying relationship.

GAM methodologies have been extensively used for identifying and analyzing complex relationships among components of climate systems (Madolli et al., 2020; Yang et al., 2005), concentration-discharge relationships (von Brömssen et al., 2023) and to investigate drivers and controls on flow-path responses and stream water nutrient concentrations (Galloway et al., 2025; Kundu et al., 2017). In our study, conducting a more detailed GAM analysis—such as incorporating varying levels of rainfall—would require a larger number of events per rainfall category, which is often a challenge in semi-arid catchments, where rainfall events are relatively infrequent.

The rainfall cluster analysis differentiates between the controls of hydrological connectivity by incorporating both event-scale characteristics (e.g., intensity, duration) and antecedent conditions. The inclusion of the ADP is highly significant, as ADP plays a key role in hydrological processes and flood estimation by influencing soil infiltration capacity and runoff generations (Grayson et al., 1997; Pathiraja et al., 2012). The majority of events with high ADP—events that occurred after prolonged dry conditions (24 out of the 32 events)—are grouped into cluster 4, which is characterized by no significant differentiation between $(SC - FC)_{sync}$ and $(SC - FC)_{seq}$. This suggests that under drier antecedent conditions, the distinction between synchronous and sequential connectivity is not apparent in the hydrological response of the system, likely due to delayed or incomplete activation of the surface flowpaths. In contrast, clusters associated with shorter ADPs show larger variance across the clusters, which indicates that likely connectivity in wetter conditions is mostly shaped and influenced by the rainfall characteristics. As it is expected that future climate patterns will change and affect the rainfall intensity and frequency, investigating in more detail the role of ADP in shaping connectivity on watershed-scale runoff is considered highly important.

Given the demonstrated differentiation of connectivity patterns under various rainfall features and ADP regimes, we also explored the potential influence of broader climatic drivers on connectivity. Specifically, we performed a preliminary clustering of SC - FC correlation patterns based on the El Niño-Southern Oscillation (ENSO) phases (El Niño, La Niña, Neutral) (Chen & Jin, 2020), which revealed small, but not negligible differences in SC - FC connectivity under the different climate patterns. The results are presented in Supporting Information S1 (Figures S5 and S6). They highlight the potential role of large-scale climate patterns in shaping hydrological connectivity and suggest a direction for future research.

4.2. Use of SC-FC Correlations in Ephemeral Systems and Beyond

Introducing SC - FC correlations in the field of hydrology and specifically in intermittent systems is a first step in advancing connectivity concepts and tools that traditionally are used in other disciplines, primarily in neuroscience. SC - FC correlations serve then as a means to quantify the extent to which the structural river network constrains or shapes the dynamic relationships of runoff behavior across the watershed.

Previous work has begun to explored SC - FC relations in hydrology and geomorphology (Turnbull & Wainwright, 2018), to compare hillslope patterns of SC and to identify hillslope locations where patterns of FC exceeded the topographically defined structurally connected pathways. In a closer parallel to the work undertaken here, Phillips et al. (2011) and Spence and Phillips (2015) explored SC - FC relations at the timescale of individual hydro-meteorological events, as a ratio of the number of edges in a river network that were connected to the outlet to the number of potential edges in the network (i.e., structural connectivity). What these approaches have in common is that they treat functional connectivity between nodes as a binary property. Tiwari et al. (2025) developed this further to explore correlations between weighted SC and FC metrics, with FC weighted by the magnitude of flow between two nodes. However, their approach was centered on the event-scale hydrological response (i.e., total event discharge at each hillslope location), so while it provided an overview of the overall connectivity of the hillslope, it does not discriminate between the timings of runoff connectivity.

The approach we use here employs one of the most classical measures to quantify FC in neuroscience, that is Pearson correlation. Pearson correlations between hydrographs capture linear statistical dependencies between the runoff timeseries and provide a methodologically simple quantification of synchronization and sequential activation between regions of the catchment. While effective in revealing how different parts of the system interact, simple correlation measures do not provide information about the causal relationships between time series—what is typically referred to in neuroscience as *effective connectivity* (Rinderer et al., 2018).

The SC - FC framework, demonstrated here, is a promising approach for understanding structural–functional connectivity relationships in intermittent hydrological systems, not only in drylands but also in a broader range of climatic regimes. In temperate and tropical regions, river connectivity varies significantly between wet and dry phases, influencing sediment transport, nutrient fluxes and species dispersal (Datry et al., 2016; Tetzlaff et al., 2015). Similarly, semi-arid monsoonal climates have a significant impact in the seasonal variability in water availability, affecting significantly hydrological and ecological connectivity (Karim et al., 2016). In cold climates, Arctic and alpine systems exhibit snowmelt-driven intermittency, which impacts sediment transport and biogeochemical cycling (Malard et al., 2006). Thawing and freezing cycles cause changes in structural connectivity and lead to corresponding periods of high and low water flow, resulting in increased variability in functional connectivity patterns, reflected in erosion processes, nutrient fluxes and microbial activity. Similar dynamics are observed in "fill and spill" systems in high-latitude environments, where temporary storage and threshold behavior in landscape depressions drive episodic connectivity (McDonnell et al., 2021; Tromp-van Meerveld & McDonnell, 2006). Likewise, "chains of ponds" systems found in drylands in Australia exhibit connectivity that is highly dependent on episodic rainfall and the spatial arrangement of ponds, reflecting both structural constraints and functional responses to hydrological inputs (Williams & Fryirs, 2020). The nature of the SC - FC framework presented in this study allows for its implementation across systems in various climatic conditions, with appropriate adaptations required to elucidate hydrological and ecological responses in each context. Such comparative studies could prove to be beneficial in disentangling the roles of geomorphology, rainfall and climatic regimes in shaping connectivity and could possibly reveal whether the observed connectivity dynamics are site- and system-specific, or representative of broader hydrological behaviors in intermittent systems. These insights could inform the development of more resilient water and land management strategies and suggest improvements in field measurement techniques (Shanafield & Cook, 2014).

Our approach is also useful for leveraging available data from gauging stations but can be also applied to continuous timeseries from hydrological models. Its simple implementation and scalability across spatial and temporal scales support its application in a variety of intermittent flow environments, such as floodplains and ephemeral river networks. Moreover, exploring further the mechanistic basis of SC - FC signatures in relation to rainfall characteristics that trigger runoff could inform decisions about where and how to deploy monitoring equipment, depending on specific research objectives. Finally, whilst we focused on temporally discrete events, separated by no-flow conditions, the approach might potentially be extended to continuous-flow systems where stormflow and baseflow hydrograph contributions are separated.

5. Conclusion

In this study, we conceptualized structural connectivity using available topographic data from WGEW, considering runoff measurement sites (flumes) as nodes within the incomplete river network. For the weighted edges, we used distance values, that is, Euclidean distance and channel lengths between the flumes. Functional connections are formed on top of this structural template as pairwise correlations between activated flumes due to runoff responses. We distinguished between synchronous functional connectivity, driven by simultaneous activation of flumes in response to rain, and sequential functional connectivity, which reflects the water propagation along the river pathways. The induced timelags in the pairwise correlations of runoff timeseries for the FC_{seq} construction were computed based on Manning's formula. The comparison between the structural and functional networks for each event revealed the degree of their similarity, quantitatively expressed by SC - FC correlations. The SC - FC relationships are also indicative of the emergent runoff patterns and their relation with rainfall features and the discharge at watershed outlet enhance the understanding of runoff dynamics across the watershed. GAM analysis with respect to the partial effects of the two types of SC - FC on the accumulated water volume at flume 1 and hierarchical clustering on rainfall features, combined with the corresponding clusters of SC - FC correlations provide insights about the interrelations between these quantities.

Our main findings suggest that: (a) larger rainfall/runoff events generally correspond to higher sequential connectivity and medium synchronous connectivity, (b) the discharge at the watershed's outlet does not exhibit linear relation to $(SC - FC)_{seq}$ correlation value, (c) the combination of high synchronous and sequential connectivity is indicative that the water reached the watershed's outlet, (d) events dominated by synchronous connectivity tend to be spatially localized, short and intense, whereas longer, lower-intensity events favor sequential connectivity. Overall, these results provide insights into local and system-scale hydrological responses, combining connectivity metrics with simple hydrological quantities. The results validate core hydrological principles, demonstrating the utility of this framework.

Conflict of Interest

The authors declare no conflicts of interest relevant to this study.

Availability Statement

The code and data used to generate the results of this study have been published on Github, https://github.com/benvoutsa/RainfallRunoffConnectivity (Benvoutsa, 2026).

Acknowledgments
This project has received funding from the European Union's Horizon 2020 research and innovation programme under the Marie Skłodowska-Curie Grant agreement No. 859937. Open Access funding enabled and organized by Projekt DEAL.

References

Baillie, M., Hogan, J., Ekwurzel, B., Wahi, A., & Eastoe, C. (2007). Quantifying water sources to a semiarid riparian ecosystem, San Pedro River, Arizona. *Journal of Geophysical Research*, *112*(G3). https://doi.org/10.1029/2006jg000263

Benda, L., & Bigelow, P. (2014). On the patterns and processes of wood in northern California streams. *Geomorphology*, *209*, 79–97. https://doi.org/10.1016/j.geomorph.2013.11.028

Benda, L., Poff, N., Miller, D., Dunne, T., Reeves, G., Pess, G., & Pollock, M. (2004). The network dynamics hypothesis: How channel networks structure riverine habitats. *BioScience*, *54*(5), 413–427. https://doi.org/10.1641/0006-3568(2004)054[0413:tndhhc]2.0.co;2

Benvoutsa. (2026). Source code runoff connectivity. *Zenodo*. https://doi.org/10.5281/zenodo.20101395

Berghuijs, W., Harrigan, S., Molnar, P., Slater, L., & Kirchner, J. (2019). The relative importance of different flood-generating mechanisms across Europe. *Water Resources Research*, *55*(6), 4582–4593. https://doi.org/10.1029/2019wr024841

Berghuijs, W., & Kirchner, J. (2020). Synchronicity and drivers of river flooding (Technical report). *Copernicus Meetings*. https://doi.org/10.5194/egusphere-egu2020-9625

Boulton, A. J., Rolls, R. J., Jaeger, K. L., & Datry, T. (2017). Hydrological connectivity in intermittent rivers and ephemeral streams. In T. Datry, N. Bonada, & A. J. Boulton (Eds.), *Intermittent rivers and ephemeral streams: Ecology and management* (pp. 79–108). Academic Press. https://doi.org/10.1016/B978-0-12-803835-2.00004-5

Briggs, L., & Krishnamoorthy, M. (2013). Exploring network scaling through variations on optimal channel networks. *Proceedings of the National Academy of Sciences*, *110*(48), 19295–19300. https://doi.org/10.1016/j.comnet.2013.03.004

Brinkerhoff, C. (2024). The importance of source data in river network connectivity modeling: A review. *Limnology and Oceanography*, *69*(12), 3033–3060. https://doi.org/10.1002/lno.12706

Bull, W. (1997). Discontinuous ephemeral streams. *Geomorphology*, *19*(3–4), 227–276. https://doi.org/10.1016/s0169-555x(97)00016-0

Chen, H., & Jin, F. (2020). Fundamental behavior of ENSO phase locking. *Journal of Climate*, *33*(5), 1953–1968. https://doi.org/10.1175/jcli-d-19-0264.1

Chouksey, A., Lambey, V., Nikam, B., Aggarwal, S., & Dutta, S. (2017). Hydrological modelling using a rainfall simulator over an experimental hillslope plot. *Hydrology*, *4*(1), 17. https://doi.org/10.3390/hydrology4010017

Crompton, O., Katul, G., Lapides, D., & Thompson, S. (2023). Bridging structural and functional hydrological connectivity in dryland ecosystems. *Catena*, *231*, 107322. https://doi.org/10.1016/j.catena.2023.107322

Czuba, J., & Foufoula-Georgiou, E. (2015). Dynamic connectivity in a fluvial network for identifying hotspots of geomorphic change. *Water Resources Research*, *51*(3), 1401–1421. https://doi.org/10.1002/2014wr016139

Datry, T., Bonada, N., & Heino, J. (2016). Towards understanding the organisation of metacommunities in highly dynamic ecological systems. *Oikos*, *125*(2), 149–159. https://doi.org/10.1111/oik.02922

Datry, T., Boulton, A. J., Fritz, K., Stubbington, R., Cid, N., Crabot, J., & Tockner, K. (2023). Non-perennial segments in river networks. *Nature Reviews Earth & Environment*, *4*(12), 815–830. https://doi.org/10.1038/s43017-023-00495-w

Deng, X., Xu, Y., Han, L., Song, S., Xu, G., & Xiang, J. (2018). Spatial-temporal changes in the longitudinal functional connectivity of river systems in the Taihu Plain, China. *Journal of Hydrology*, *566*, 846–859. https://doi.org/10.1016/j.jhydrol.2018.09.060

Dwivedi, D., Poeppl, R., & Wohl, E. (2025). Hydrological connectivity: A review and emerging strategies for integrating measurement, modeling, and management. *Frontiers in Water*, *7*, 1496199. https://doi.org/10.1002/hyp.70131

Freeze, R. (1980). A stochastic-conceptual analysis of rainfall-runoff processes on a hillslope. *Water Resources Research*, *16*(2), 391–408. https://doi.org/10.1029/wr016i002p00391

Galloway, J., Ezzati, G., Hawtree, D., Richards, K., Lynch, B., Burgess, E., et al. (2025). Using generalized additive models to investigate drivers and controls on stream water nitrate concentrations in four agricultural catchments. *Agricultural Water Management*, *315*, 109552. https://doi.org/10.1016/j.agwat.2025.109552

Garbin, S., Celegon, E. A., Fanton, P., & Botter, G. (2019). Hydrological controls on river network connectivity. *Royal Society open science*, *6*(2), 181428. https://doi.org/10.1098/rsos.181428

Goodrich, D., Lane, L., Shillito, R., Miller, S., Syed, K., & Woolhiser, D. (1997). Linearity of basin response as a function of scale in a semiarid watershed. *Water resources research*, *33*(12), 2951–2965. https://doi.org/10.1029/97wr01422

Goodrich, D., Williams, D., Unkrich, C., Hogan, J., Scott, R., Hultine, K., et al. (2004). Comparison of methods to estimate ephemeral channel recharge, Walnut Gulch, San Pedro River basin, Arizona. Groundwater recharge in a desert environment. *The southwestern United States*, *9*, 77–99. https://doi.org/10.1029/009wsa06

Goodrich, J.-M., Woolhiser, D. A., Lane, L. J., & Sorooshian, S. (1995). Measurement and analysis of small-scale convective storm rainfall variability. *Journal of hydrology*, *173*(1–4), 283–308. https://doi.org/10.1016/0022-1694(95)02703-r

Goodrich, D. C., Keefer, T., Unkrich, C., Nichols, M., Osborn, H., Stone, J., & Smith, J. (2008). Long-term precipitation database, Walnut Gulch Experimental Watershed, Arizona, United States. *Water Resources Research*, *44*(5). https://doi.org/10.1029/2006WR005782

Goodrich, D. C., Kepner, W., Levick, L., & Wigington Jr, P. (2018). Southwestern intermittent and ephemeral stream connectivity. *JAWRA Journal of the American Water Resources Association*, *54*(2), 400–422. https://doi.org/10.1111/1752-1688.12636

Grayson, R., Western, A., Chiew, F., & Blöschl, G. (1997). Preferred states in spatial soil moisture patterns: Local and nonlocal controls. *Water resources research*, *33*(12), 2897–2908. https://doi.org/10.1029/97wr02174

Harvey, J., Gomez-Velez, J., Schmadel, N., Scott, D., Boyer, E., Alexander, R., et al. (2019). How hydrologic connectivity regulates water quality in river corridors. *JAWRA Journal of the American Water Resources Association*, *55*(2), 369–381. https://doi.org/10.1111/1752-1688.12691

Heilman, P., Nichols, M., Goodrich, D., Miller, S., & Guertin, D. (2008). Geographic information systems database, walnut gulch experimental watershed, Arizona, United States. *Water resources research*, *44*(5). https://doi.org/10.1029/2006wr005777

Hooke, J. (2016). Morphological impacts of flow events of varying magnitude on ephemeral channels in a semiarid region. *Geomorphology*, *252*, 128–143. https://doi.org/10.1016/j.geomorph.2015.07.014

Hooke, J. (2022). Morphodynamics of a meandering channel over decadal timescales in response to hydrological variations. *Earth Surface Processes and Landforms*, *47*(8), 1902–1920. https://doi.org/10.1002/esp.5354

Howard, A., Keetch, M., & Vincent, G. (1970). Topological and geometrical properties of braided streams. *Water Resources Research*, *6*(6), 1674–1688. https://doi.org/10.1029/wr006i006p01674

Iddrisu, W. A., Nokoe, K. S., Luguterah, A., & Antwi, E. O. (2017). Generalized additive mixed modelling of river discharge in the black Volta river. *Open Journal of Statistics*, *7*(4), 621–632. https://doi.org/10.4236/ojs.2017.74043

Karim, F., Petheram, C., Marvanek, S., Ticehurst, C., Wallace, J., & Hasan, M. (2016). Impact of climate change on floodplain inundation and hydrological connectivity between wetlands and rivers in a tropical river catchment. *Hydrological ocesses*, *30*(10), 1574–1593. https://doi.org/10.1002/hyp.10714

Khatami, S., Peel, M., Peterson, T., & Western, A. (2019). Equifinality and flux mapping: A new approach to model evaluation and process representation under uncertainty. *Water Resources Research*, *55*(11), 8922–8941. https://doi.org/10.1029/2018wr023750

Kundu, D., Vervoort, R. W., & van Ogtrop and, F. F. (2017). Inferring catchment flow path responses using a data-driven model: An exploratory study based on a generalized additive model. *Hydrological Sciences Journal*, *62*(12), 1965–1979. https://doi.org/10.1080/02626667.2017.1357887

Letcher, R., Schreider, S., Jakeman, A., Neal, B., & Nathan, R. (2001). Methods for the analysis of trends in streamflow response due to changes in catchment condition. *Environmetrics*, *12*(7), 613–630. https://doi.org/10.1002/env.486

Lu, M., Hua, J., Yu, Z., & Xu, Y. (2024). Towards transient connectivity of river networks during rainfall events: Insight from hydrological observation and functional data analysis. *Journal of Hydrology*, *637*(131366), 131366. https://doi.org/10.1016/j.jhydrol.2024.131366

Madolli, M., Madolli, U., Sangreskop, H., & Pa, G. (2020). The application of generalized additive models (GAMs) for assessing the teleconnection of ENSO and IOD with monsoon rainfall variability over Krishna river basin, India. *Journal of Agrometeorology*, *22*(1), 33–40.

Malard, F., Uehlinger, U., Zah, R., & Tockner, K. (2006). Flood-pulse and riverscape dynamics in a braided glacial river. *Ecology*, *87*(3), 704–716. https://doi.org/10.1890/04-0889

McDonnell, J., Spence, C., Karran, D., Van Meerveld, H., & Harman, C. (2021). Fill-and-spill: A process description of runoff generation at the scale of the beholder. *Water Resources Research*, *57*(5), e2020WR027514. https://doi.org/10.1029/2020wr027514

Meles, M., Bradford, S., Casillas-Trasvina, A., Chen, L., Osterman, G., Hatch, T., et al. (2024). Uncovering the gaps in managed aquifer recharge for sustainable groundwater management: A focus on hillslopes and mountains. *Journal of Hydrology*, *639*, 131615. https://doi.org/10.1016/j.jhydrol.2024.131615

Meles, M., Demaria, E., Heilman, P., Goodrich, D., Kautz, M., Armendariz, G., et al. (2022). Curating 62 years of walnut gulch experimental watershed data: Improving the quality of long-term rainfall and runoff datasets. *Water*, *14*(14), 2198. https://doi.org/10.3390/w14142198

Merz, R., & Blöschl, G. (2003). A process typology of regional floods. *Water resources research*, *39*(12). https://doi.org/10.1029/2002wr001952

Msilini, A., Charron, C., Ouarda, T., & Masselot, P. (2022). Flood frequency analysis at ungauged catchments with the GAM and MARS approaches in the Montreal region, Canada. *Canadian Water Resources Journal/Revue canadienne des ressources hydriques*, *47*(2–3), 111–121. https://doi.org/10.1080/07011784.2022.2044385

Nichols, M. (2019). 15: The walnut gulch experimental Watershed—50 years of watershed monitoring and research. In *Monitoring and evaluation of soil conservation and watershed development projects* (pp. 267–278). CRC Press. https://doi.org/10.1061/40928(251)12

Nichols, M., & Anson, E. (2008). Southwest watershed research Center data access project. *Water Resources Research*, *44*(5). https://doi.org/10.1029/2006WR005665

Ouarda, T., Charron, C., Hundecha, Y., St-Hilaire, A., & Chebana, F. (2018). Introduction of the GAM model for regional low-flow frequency analysis at ungauged basins and comparison with commonly used approaches. *Environmental modelling & software*, *109*, 256–271. https://doi.org/10.1016/j.envsoft.2018.08.031

Parsons, A., Pöppl, R., & Keesstra, S. (2025). Connectivity in geomorphology. In *Chap. Connectivity concepts*. Cambridge University Press. https://doi.org/10.1017/9781108903196

Passalaqua, P. (2016). The delta connectome: A network-based framework for studying connectivity in river deltas. *Geomorphology*, *277*, 50–62. https://doi.org/10.1016/j.geomorph.2016.04.001

Pathiraja, S., Westra, S., & Sharma, A. (2012). Why continuous simulation? The role of antecedent moisture in design flood estimation. *Water Resources Research*, *48*(6). https://doi.org/10.1029/2011wr010997

Peron, T., Comin, C., Amancio, D., Costa, L., Rodrigues, F., & Kurths, J. (2014). Correlations between climate network and relief data. *Nonlinear Processes in Geophysics*, *21*, 1127–1132. https://doi.org/10.5194/npgd-1-823-2014

Phillips, R., Spence, C., & Pomeroy, J. (2011). Connectivity and runoff dynamics in heterogeneous basins. *Hydrological Processes*, *121*, 3061–3075. https://doi.org/10.5194/hess-2022-102

Ran, X., Xi, Y., Lu, Y., Wang, X., & Lu, Z. (2023). Comprehensive survey on hierarchical clustering algorithms and the recent developments. *Artificial Intelligence Review*, *56*(8), 8219–8264. https://doi.org/10.3233/faia190176

Rashid, M., & Beecham, S. (2019). Simulation of streamflow with statistically downscaled daily rainfall using a hybrid of wavelet and GAMLSS models. *Hydrological Sciences Journal*, *64*(11), 1327–1339. https://doi.org/10.1080/02626667.2019.1630742

Recinos, S., Funk, A., Tiwari, S., Baldan, D., & Hein, T. (2024). Multilayer networks in landscape ecology: A case study to assess changes in aquatic habitat connectivity for flying and non-flying benthic macroinvertebrates in a Danube floodplain. *Landscape Ecology*, *39*(11), 1–27. https://doi.org/10.1007/s10980-024-01975-0

Rigon, R., Rinaldo, A., Rodriguez-Iturbe, I., Bras, R., & Ijjasz-Vasquez, E. (1993). Optimal channel networks: A framework for the study of river basin morphology. *Water Resources Research*, *29*(6), 1635–1646. https://doi.org/10.1029/92wr02985

Rinderer, M., Ali, G., & Larsen, L. (2018). Assessing structural, functional and effective hydrologic connectivity with brain neuroscience methods: State-of-the-art and research directions. *Earth-Science Reviews*, *178*, 29–47. https://doi.org/10.1016/j.earscirev.2018.01.009

Sendrowski, A., & Passalacqua, P. (2017). Process connectivity in a naturally prograding river delta. *Water Resources Research*, *53*(3), 1841–1863. https://doi.org/10.1002/2016wr019768

Shanafield, M., & Cook, P. (2014). Transmission losses, infiltration and groundwater recharge through ephemeral and intermittent streambeds: A review of applied methods. *Journal of Hydrology*, *511*, 518–529. https://doi.org/10.1016/j.jhydrol.2014.01.068

Sheppard, D., Tomberlin, J., Joyce, J., Kiser, B., & Sumner, S. (2002). Rearing methods for the black soldier fly (Diptera: Stratiomyidae). *Journal of medical entomology*, *39*(4), 695–698. https://doi.org/10.1603/0022-2585-39.4.695

Sivakumar, B., & Singh, V. (2012). Hydrologic system complexity and nonlinear dynamic concepts for a catchment classification framework. *Hydrology and Earth System Sciences*, *16*(11), 4119–4131. https://doi.org/10.5194/hessd-8-4427-2011

Snyder, K., & Williams, D. (2000). Water sources used by riparian trees varies among stream types on the San Pedro River, Arizona. *Agricultural and Forest Meteorology*, *105*(1–3), 227–240. https://doi.org/10.1016/s0168-1923(00)00193-3

Spence, C., & Phillips, R. (2015). Refining understanding of hydrological connectivity in a boreal catchment. *Hydrological Processes*, *29*(16), 3491–3503. https://doi.org/10.1002/hyp.10270

Tejedor, A., Longjas, A., Zaliapin, I., & Foufoula-Georgiou, E. (2015). Delta channel networks: 1. A graph-theoretic approach for studying connectivity and steady state transport on deltaic surfaces. *Water Resources Research*, *51*(6), 3998–4018. https://doi.org/10.1002/2014wr016577

Tetzlaff, D., Buttle, J., Carey, S., McGuire, K., Laudon, H., & Soulsby, C. (2015). Tracer-based assessment of flow paths, storage and runoff generation in northern catchments: A review. *Hydrological Processes*, *29*(16), 3475–3490. https://doi.org/10.1002/hyp.10412

Tiwari, S., Brizuela, S., Hein, T., Turnbull, L., Wainwright, J., & Funk, A. (2024). Water-controlled ecosystems as complex networks: Evaluation of network-based approaches to quantify patterns of connectivity. *Ecohydrology*, *17*(7), e2690. https://doi.org/10.22541/au.168674584.45045056/v1

Tiwari, S., Turnbull, L., & Wainwright, J. (2025). Local-and global-scale hydrological and sediment connectivity over grassland and shrubland hillslopes. *Journal of Hydrology*, *655*(132896). https://doi.org/10.22541/essoar.172118419.91181383/v1

Tromp-van Meerveld, H., & McDonnell, J. (2006). Threshold relations in subsurface stormflow: 2. The fill and spill hypothesis. *Water resources research*, *42*(2). https://doi.org/10.1029/2004wr003800

Turnbull, L., Hütt, M.-T., Ioannides, A. A., Kininmonth, S., Poeppl, R., Tockner, K., et al. (2018). Connectivity and complex systems: Learning from a multi-disciplinary perspective. *Applied Network Science*, *3*, 1–49. https://doi.org/10.1007/s41109-018-0067-2

Turnbull, L., & Wainwright, J. (2018). From structure to function: Understanding shrub encroachment in drylands using hydrological and sediment connectivity. *Ecological Indicators*, *98*, 608–618. https://doi.org/10.1016/j.ecolind.2018.11.039

USDA Agricultural Research Service, Southwest Watershed Research Center. (2025). SWRC data access project. https://doi.org/10.1029/2006wr005665

von Brömssen, C., Fölster, J., Kyllmar, K., & Bieroza, M. (2023). Modeling complex concentration-discharge relationships with generalized additive models. *Environmental Modeling & Assessment*, *28*(6), 925–937. https://doi.org/10.1007/s10666-023-09915-z

Voutsa, V., Battaglia, D., Bracken, L., Brovelli, A., Costescu, J., Diaz Munoz, M., et al. (2021). Two classes of functional connectivity in dynamical processes in networks. *Journal of the Royal Society Interface*, *18*(183), 20210486. https://doi.org/10.1098/rsif.2021.0486

Wainwright, J., Parsons, A. J., Schlesinger, W. H., & Abrahams, A. D. (2002). Hydrology–vegetation interactions in areas of discontinuous flow on a semi-arid bajada, southern New Mexico. *Journal of Arid Environments*, *51*(3), 319–338. https://doi.org/10.1006/jare.2002.0970

Wainwright, J., Turnbull, L., Ibrahim, T., Lexartza-Artza, I., Thornton, S., & Brazier, R. (2011). Linking environmental régimes, space and time: Interpretations of structural and functional connectivity. *Geomorphology*, *126*(3–4), 387–404. https://doi.org/10.1016/j.geomorph.2010.07.027

henation="11">Williams, R., & Fryirs, K. (2020). The morphology and geomorphic evolution of a large chain-of-ponds river system. *Earth Surface Processes and Landforms*, *45*(8), 1732–1748. https://doi.org/10.1002/esp.4842

Wohl, E. (2017). Connectivity in rivers. *Progress in Physical Geography*, *41*(3), 345–362. https://doi.org/10.1177/0309133317714972

Xu, J., Li, W., Ji, M., Lu, F., & Dong, S. (2010). A comprehensive approach to characterization of the nonlinearity of runoff in the headwaters of the Tarim River, western China. *Hydrological Processes: An International Journal*, *24*(2), 136–146. https://doi.org/10.1002/hyp.7484

Yang, C., Chandler, R., Isham, V., & Wheater, H. (2005). Spatial-temporal rainfall simulation using generalized linear models. *Water Resources Research*, *41*(11). https://doi.org/10.1029/2004wr003739

Zanetti, F., Botter, G., & Camporese, M. (2024). Stream network dynamics of non-perennial rivers: Insights from integrated surface-subsurface hydrological modeling of two virtual catchments. *Water Resources Research*, *60*(2), e2023WR035631. https://doi.org/10.1029/2023wr035631

Zhao, X., Ma, X., Chen, B., Shang, Y., & Song, M. (2022). Challenges toward carbon neutrality in China: Strategies and countermeasures. *Resources, Conservation and Recycling*, *176*, 105959. https://doi.org/10.1016/j.resconrec.2021.105959